1 H), 6.60 (s, 1 H), 7.64 (s, 1 H); chemical ionization mass spectrum, *m/e* 655.4347 (MH^+, calcd for $C_{39}H_{63}O_6Si$, 655.4377).

2,5,6,7-Tetradehydro-7,28-dideoxy-25-methyl-(25*R*)-(±)-milbemycin B (42a). Diene **40a** (65 mg, 0.098 mmol) was dissolved in 5 mL of THF and excess (ca. 2 mL, 1 M) Bu_4NF–THF (Aldrich) solution added. The orange solution was stirred for 4 h at 25 °C. Water was then added and the mixture extracted with ether; the ether fractions were washed with brine, dried over $MgSO_4$, and evaporated. The resultant alcohol was dissolved in 10 mL of THF and added to five drops (excess) of a 35% KH–oil dispersion (previously, washed with ether) in 10 mL of THF. The mixture was stirred at 25 °C for 3 h. Saturated NH_4Cl was then added and the mixture extracted with ether; the ether solution was washed with brine, dried over $MgSO_4$, and evaporated. Purification by flash chromatography [hexane–ethyl acetate, 30:1 (v/v)] afforded 38 mg (76%) of macrolide **42a** as a colorless viscous oil: IR (CCl_4) 2940 (br s), 1715 (s), 1605 (m), 1550 (w), 1265 (br s), 1170 (s), 1105 (s), 1055 (s), 1005 (s), 970 (m), 855 (w) cm^{-1}; ^1H NMR (250 MHz, $CDCl_3$) δ 0.70–2.38 (m, 13 H), 0.82 (d, *J* = 6.3 Hz, 3 H), 1.02 (d, *J* = 6.6 Hz, 3 H), 1.12 (d, *J* = 6.3 Hz, 3 H), 1.62 (s, 3 H), 2.09 (s, 3 H), 2.17 (s, 3 H), 2.48 (m, 1 H), 3.27 (m, 1 H), 3.67 (m, 1 H), 3.82 (s, 3 H), 4.88 (br d, *J* = 8.8 Hz, 1 H), 5.24 (dd, *J* = 14.9, 9.4 Hz, 1 H), 5.50 (m, 1 H), 5.70 (d, *J* = 10.7 Hz, 1 H), 6.12 (dd, *J* = 14.9, 10.7 Hz, 1 H), 6.60 (s, 1 H), 7.32 (s, 1 H); chemical ionization mass spectrum, *m/e* 509.3237 (MH^+, calcd for $C_{32}H_{45}O_5$, 509.3255).

In a similar manner diene **40b** (89 mg, 0.135 mmol) was converted into macrolide **42b** (54 mg, 79%): IR (CCl_4) 2930 (br s), 1700 (s), 1600 (m), 1265 (br s), 1170 (s), 1050 (m), 1000 (m), 960 (w), 850 (w) cm^{-1}; ^1H NMR (250 MHz, $CDCl_3$) δ 0.75–2.32 (m, 13 H), 0.82 (d, *J* = 6.6 Hz, 3 H), 1.06 (d, *J* = 6.6 Hz, 3 H), 1.12 (d, *J* = 6.2 Hz, 3 H), 1.60 (s, 3 H), 2.02 (s, 3 H), 2.16 (s, 3 H), 2.50 (m, 1 H), 3.22 (dq, *J* = 9.8, 7.0 Hz, 1 H), 3.73 (m, 1 H), 3.80 (s, 3 H), 5.16 (br d, *J* = 10.6 Hz, 1 H), 5.28 (m, 1 H), 5.42 (dd, *J* = 15.1, 8.9 Hz, 1 H), 5.80 (d, *J* = 10.8 Hz, 1 H), 6.15 (dd, *J* = 15.1, 10.8 Hz, 1 H), 6.58 (s, 1 H), 7.32 (s, 1 H); chemical ionization mass spectrum, *m/e* 509.3231 (MH^+, calcd for $C_{32}H_{45}O_5$, 509.3255).

Milbemycin β_3 (1a) and Its Epimer, Epimilbemycin β_3 (1b). Sodium hydride (400 mg, 60% oil dispersion) was washed with ether under argon and dried. Distilled DMF (5 mL) was added, followed by careful addition of sufficient 1:1 EtSH–DMF to consume all of the hydride. Methyl ether **42a** (37 mg, 0.073 mmol) in 5 mL of DMF was then added to the clear yellow solution and the mixture heated at reflux for 1 h. The reaction mixture was cooled, poured into saturated NH_4Cl, and extracted with ether. The ether extract was washed with water and brine, dried over $MgSO_4$, and concentrated in vacuo. Purification by flash chromatography [hexane–ethyl acetate, 5:1 (v/v)] afforded 31 mg (84%) of milbemycin β_3 (**1**) as a colorless hard glass. Crystallization from methylene chloride–hexane afforded 29 mg of crystalline solid: mp 153–156 °C; IR (CCl_4), 3600 (w), 3470 (br), 2940 (br s), 1675 (s), 1605 (m), 1285 (s), 1170 (s), 995 (s), 965 (m) cm^{-1}; ^1H NMR (250 MHz, $CDCl_3$) δ 0.65–2.35 (m, 13 H), 0.82 (d, *J* = 6.6 Hz, 3 H), 1.00 (d, *J* = 6.6 Hz, 3 H), 1.12 (d, *J* = 6.3 Hz, 3 H), 1.61 (s, 3 H), 2.04 (s, 3 H), 2.20 (s, 3 H), 2.45 (m, 1 H), 3.26 (dq, *J* = 9.8, 7 Hz, 1 H), 3.68 (m, 1 H), 4.87 (br d, *J* = 9.5 Hz, 1 H), 5.13 (s, 1 H), 5.23 (dd, *J* = 15.1, 9.5 Hz, 1 H), 5.49 (m, 1 H), 5.69 (d, *J* = 11.1 Hz, 1 H), 6.12 (dd, *J* = 15.1, 11.1 Hz, 1 H), 6.59 (s, 1 H), 7.30 (s, 1 H); ^{13}C NMR (62.5 MHz, $CDCl_3$) δ 15.19, 16.10, 17.83, 18.01, 19.39, 21.63, 27.83, 33.89, 35.83, 36.30, 36.62, 41.27, 48.74, 67.68, 68.21, 71.24, 97.73, 114.23, 121.52, 122.38, 124.11, 125.49, 128.79, 131.93, 134.05, 135.78, 140.26, 144.20, 155.55, 169.52.

Anal. Calcd for $C_{31}H_{42}O_5$: C, 75.27; H, 8.56. Found: C, 75.09; H, 8.77.

In a similar manner macrolide **42b** (50 mg, 0.098 mmol) was converted into **1b** (42.7 mg, 88%): mp 221–224 °C dec; IR (CCl_4), 3600 (w), 3470 (br), 2940 (br s), 1670 (s), 1601 (m), 1290 (s), 1175 (s), 1005 (s), 965 (m) cm^{-1}; ^1H NMR (250 MHz, $CDCl_3$) δ 0.75–2.30 (m, 13 H), 0.80 (d, *J* = 6.6 Hz, 3 H), 1.04 (d, *J* = 7.0 Hz, 3 H), 1.09 (d, *J* = 6.3 Hz, 3 H), 1.58 (s, 3 H), 1.98 (s, 3 H), 2.20 (s, 3 H), 2.47 (m, 1 H), 3.23 (dq, *J* = 10.0, 7.5 Hz, 1 H), 3.75 (br d, *J* = 10.7 Hz, 1 H), 5.15 (br d, *J* = 12.9 Hz, 1 H), 5.25 (m, 1 H), 5.40 (dd, *J* = 15.3, 9.2 Hz, 1 H), 5.52 (s, 1 H), 5.76 (d, *J* = 10.7 Hz, 1 H), 6.12 (dd, *J* = 15.3, 10.7 Hz, 1 H), 6.53 (s, 1 H), 7.28 (s, 1 H); ^{13}C NMR (62.5 MHz, $CDCl_3$) δ 15.13, 15.92, 17.86, 18.86, 19.33, 21.86, 27.92, 32.60, 34.27, 35.45, 35.77, 36.62, 40.83, 48.48, 66.12, 69.50, 71.18, 97.53, 114.85, 121.58, 122.20, 124.41, 125.17, 128.64, 131.52, 134.87, 135.29, 140.05, 144.87, 155.61, 168.75; chemical ionization mass spectrum, *m/e* 495.3070 (MH^+, calcd for $C_{31}H_{43}O_5$, 495.3099).

Acknowledgment. It is a pleasure to acknowledge the support of this investigation by the National Institutes of Health (Institute of General Medical Sciences) through Grant GM-29028 and by Merck, Sharp & Dohme Research Laboratories. In addition, we thank S. T. Bella of the Rockefeller University for the microanalyses and Drs. G. Furst, T. Terwilliger, and J. Dykins of the University of Pennsylvania Spectroscopic Service Centers for aid in recovering and interpreting the high-field NMR and mass spectra.

Photocycloaddition of Anthracene to *trans,trans*-2,4-Hexadiene

Jack Saltiel,* Reza Dabestani, Kirk S. Schanze, Deanna Trojan, David E. Townsend, and Virgil L. Goedken

Contribution from the Department of Chemistry, The Florida State University, Tallahassee, Florida 32306. *Received October 10, 1985*

Abstract: Irradiation of anthracene (A) in the presence of *trans,trans*-2,4-hexadiene (D) gives A dimer (A_2), two adducts corresponding to [4 + 4] addition of D to the 9,10 positions of A, an adduct corresponding to [2 + 4] addition, and several unidentified minor adducts. A-^{14}C and isotopic dilution based analyses were used to establish that D reduces rather than enhances anthracene photodimerization quantum yields. A thermal Diels–Alder reaction between the strained trans double bond of the major anthracene/diene adduct (*t*-[4,4]Ad) and A is shown to account quantitatively for high A losses previously attributed to A dimerization. The structure of the 2:1 A/D adduct (A_2d) and, by inference, the structure of *t*-[4,4]Ad are established unequivocally by X-ray crystallography. These observations confirm Kaupp's qualitative results and conclusions. The singlet A/D exciplex is not an intermediate leading to either anthracene dimer or to A_2d. The singlet pathway for adducts gives *t*-[4,4]Ad (81%), *c*-[4,4]Ad (<5%), and the [2 + 4] adduct ([2,4]Ad) (14%). Triplet quenching, sensitization, and CH_3I experiments show that [2,4]-Ad and a fourth unknown minor adduct (x-Ad) derive from triplet-state precursors.

Suzuki was the first to propose that a termolecular interaction may enhance the efficiency of anthracene (A) photodimer (A_2) formation in solution.[1] In modern notation,[2,3] he proposed that interaction between the singlet anthracene excimer, $^1(AA)^*$, and anthracene gives A_2.

$$^1(AA)^* + A \rightarrow A_2 + A \quad (1)$$

Although eq 1 has been shown not to explain Suzuki's observations[4] which furthermore were not borne out by recent experi-

(1) Suzuki, M. *Bull. Chem. Soc. Jpn.* **1950**, *23*, 120.
(2) Bowen, E. J. *Adv. Photochem.* **1963**, *1*, 23.
(3) Stevens, B. *Adv. Photochem.* **1971**, *8*, 161.

0002-7863/86/1508-2674$01.50/0

ments,[4,5] termolecular processes leading to A_2 have been suggested to account for enhanced anthracene loss in the presence of 1,3-dienes.[6,7] Liu, who reported that 9-phenylanthracene gave photodimer only in the presence of 1,3-dienes,[6a] D, favored an excimer mediated mechanism[6b]

$$^1(AA)^* + D \rightarrow A_2 + D \quad (2)$$

which is analogous to eq 1, whereas we suggested an exciplex mediated mechanism[7]

$$^1(AD)^* + A \rightarrow A_2 + D \quad (3)$$

for the anthracene/*trans,trans*-2,4-hexadiene system. Later we presented evidence for a photodimer formation path involving the long-lived anthracene/*N,N*-dimethylaniline singlet exciplex,[4] and others[8,9] proposed similar steps for photochemical reactants other than anthracenes. Finally, the quenching of exciplex fluorescence by specific quenchers[10] and the observation of fluorescence from trimolecular species,[11,12] triplexes,[12] or exterplexes[13] suggested that eq 2 and 3 may provide viable pathways to photoproducts.

The importance of eq 2 and 3 as product-forming steps, at least in anthracene/1,3-diene systems, has been questioned recently by Kaupp.[14] Kaupp showed that claims to the contrary notwithstanding,[6,15] 9-phenylanthracene photodimerizes more efficiently in pure benzene than when 1,3-dienes are present.[14] Similarly, it was shown that D reduces rather than enhances A_2 formation.[14] Three A/D photoadducts were identified:[14] the major [4 + 4] adduct *t*-[4,4]Ad with a strained trans double bond, which was first reported by Yang,[16] and two minor adducts, *c*-[4,4]Ad and [2,4]Ad, the first of which had been reported by Yang as a secondary photoproduct obtained from the xanthone-sensitized trans–cis isomerization of *t*-[4,4]Ad.[16] Kaupp furthermore claimed that on standing *t*-[4,4]Ad undergoes thermal Diels–Alder reaction with A to give the 2:1 adduct A_2d. It was concluded that anthracene–diene adduct formation accounted entirely for diene-enhanced anthracene losses.[14]

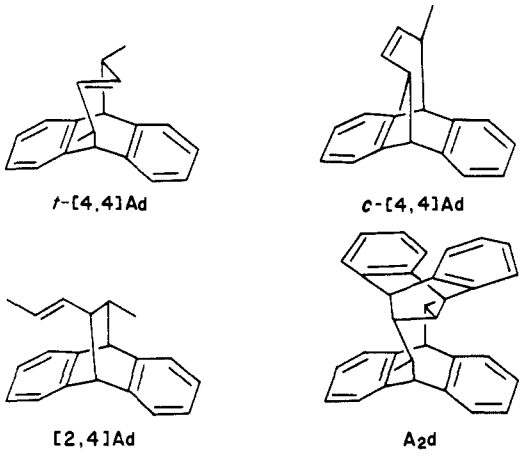

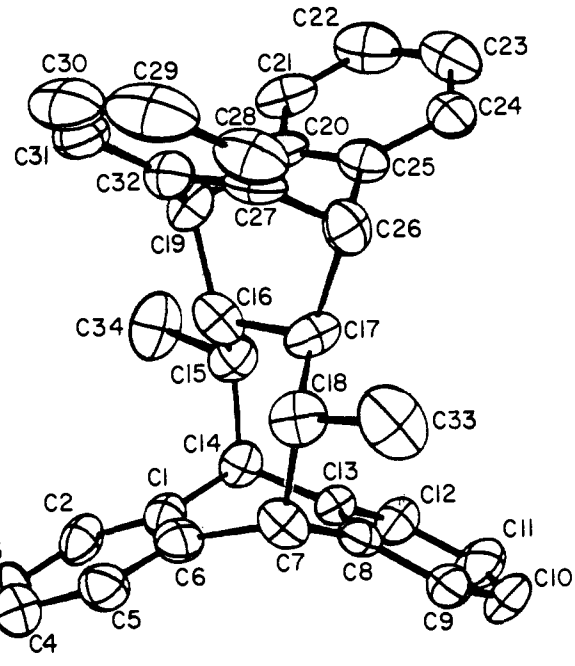

Figure 1. Ortep drawing of A_2d.

Since Kaupp's observations were largely qualitative and not based on a rigorous kinetics treatment we undertook a quantitative study of photocycloaddition in the A/D system. We sought to determine whether the 1:1 A/D adducts have common or different precursors and whether there is any validity to eq 3 as an A_2-forming step in this system. The results of this work confirm quantitatively Kaupp's conclusions showing clearly that exciplex/anthracene interactions are not involved in either A_2 or A_2d formation.

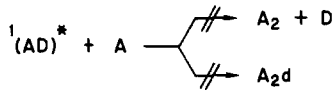

Results

Photochemical Observations. (A) Preparative. Preparative irradiations were carried out in benzene or *n*-pentane by using conditions similar to those reported by Yang and Libman.[16] The relative yield of A_2 increases with [A], but cross-adduct distributions, determined by ^{1}H NMR spectroscopy, were remarkably independent of both [A] (6.0×10^{-4}–4.0×10^{-2} M) and [D] (0.09–0.8 M) when irradiated solutions were deaerated with Ar. Adduct distributions were also independent of light intensity (200- and 450-W Hanovia Hg lamps were employed) and of the presence of a Uranium glass filter in addition to Pyrex. The ranges of adduct distributions observed were 75–86% *t*-[4,4]Ad, 3.5–5.5% *c*-[4,4]Ad, and 11–18% [2,4]Ad. A typical experiment with $[A]_0 = 2.60 \times 10^{-2}$ M and [D] = 0.8 M gave the three adducts in 85.2, 3.7, and 11.1%, in the same order. Little or no A_2d ($\leq$3%) was present in reaction mixtures requiring <2 h of irradiation for complete A consumption. As will be shown below, these adduct distributions reflect mainly the singlet reaction pathway. Product mixtures rich in *c*-[4,4]Ad were obtained by quantitative xanthone-sensitized isomerization of *t*-[4,4]Ad as previously reported.[16] This sensitized trans–cis reaction proceeds only if D is removed from the reaction mixture obtained by direct excitation prior to xanthone addition. Mixtures rich in [2,4]Ad were obtained from the fluorenone-sensitized addition of ^{3}A* to D. Neither [4 + 4] adduct is observed in NMR spectra of such reaction mixtures in which [2,4]Ad appears as the major cross-adduct. Nonetheless, sensitized reaction mixtures obtained following complete A loss are rather complex, probably due mainly to the presence of several geometric isomers of [2,4]Ad, resulting in part because D completes for fluorenone triplets and undergoes extensive trans–cis isomerization. NMR spectra of the three adducts agreed well

(4) Saltiel, J.; Townsend, D. E.; Watson, B. D.; Shannon, P.; Finson, S. L. *J. Am. Chem. Soc.* **1977**, *99*, 884.
(5) Saltiel, J.; Dabestani, R.; Charlton, J. L. *J. Am. Chem. Soc.* **1983**, *105*, 3473.
(6) (a) Campbell, R. O.; Liu, R. S. H. *Chem. Commun.* **1970**, 1191. (b) Campbell, R. O.; Liu, R. S. H. *Mol. Photochem.* **1974**, *6*, 207.
(7) Saltiel, J.; Townsend, D. E. *J. Am. Chem. Soc.* **1973**, *95*, 6140.
(8) Wells, P. P.; Morrison, H. *J. Am. Chem. Soc.* **1975**, *97*, 154.
(9) Green, B. S.; Rejto, M.; Johnson, D. E.; Hoyle, C. E.; Simpson, J. T.; Correa, P. E.; Ho, T.-I.; McCoy, F.; Lewis, F. D. *J. Am. Chem. Soc.* **1979**, *100*, 3325.
(10) For a review see: Caldwell, R. A.; Creed, D. *Acc. Chem. Res.* **1980**, *13*, 45.
(11) Beens, H.; Weller, A. *Chem. Phys. Lett.* **1968**, *2*, 140.
(12) Saltiel, J.; Townsend, D. E.; Watson, B. D.; Shannon, P. *J. Am. Chem. Soc.* **1975**, *97*, 5688.
(13) Creed, D.; Caldwell, R. A. *J. Am. Chem. Soc.* **1974**, *96*, 7369.
(14) Kaupp, G.; Teufel, E. *Chem. Ber.* **1980**, *113*, 3669.
(15) (a) Calas, R.; Lalande, R. *Bull. Soc. Chim. Fr.* **1959**, 766. (b) Bouas-Laurent, H.; Lapouyade, R.; Faugere, J. *Compt. Rend.* **1967**, *265C*, 506.
(16) Yang, N. C.; Libman, J. *J. Am. Chem. Soc.* **1972**, *94*, 1405.

Table I. Positional Parameters for Carbon Atoms in A_2d[a]

atom	x	y	z
C1	0.3858 (6)	-0.0244 (4)	0.8098 (4)
C2	0.3093 (6)	0.0273 (4)	0.8499 (4)
C3	0.2992 (6)	0.1128 (4)	0.8315 (4)
C4	0.3575 (6)	0.1443 (4)	0.7706 (4)
C5	0.4339 (4)	0.0935 (3)	0.7321 (4)
C6	0.4508 (5)	0.0109 (4)	0.7515 (3)
C7	0.5493 (6)	-0.0446 (4)	0.7169 (3)
C8	0.6260 (5)	-0.1083 (3)	0.7874 (3)
C9	0.7687 (6)	-0.1279 (4)	0.8029 (4)
C10	0.8343 (5)	-0.1828 (4)	0.8690 (4)
C11	0.7603 (6)	-0.2199 (5)	0.9191 (4)
C12	0.6211 (6)	-0.1994 (3)	0.9046 (4)
C13	0.5500 (5)	-0.1444 (4)	0.8391 (3)
C14	0.3988 (6)	-0.1169 (3)	0.8268 (4)
C15	0.2802 (5)	-0.1676 (4)	0.7598 (4)
C16	0.2572 (7)	-0.1421 (5)	0.6645 (3)
C17	0.3906 (5)	-0.1625 (4)	0.6313 (3)
C18	0.4749 (6)	-0.0872 (4)	0.6247 (4)
C19	0.1187 (5)	-0.1805 (4)	0.5939 (3)
C20	0.1463 (6)	-0.2743 (4)	0.5885 (3)
C21	0.0665 (5)	-0.3382 (5)	0.6077 (3)
C22	0.0993 (6)	-0.4194 (5)	0.5955 (4)
C23	0.2174 (7)	-0.4378 (5)	0.5707 (3)
C24	0.3004 (5)	-0.3739 (4)	0.5543 (3)
C25	0.2626 (6)	-0.2920 (4)	0.5609 (3)
C25	0.3353 (6)	-0.2156 (4)	0.5416 (4)
C27	0.2256 (5)	-0.1621 (4)	0.4746 (3)
C28	0.2323 (7)	-0.1327 (4)	0.3942 (4)
C29	0.1184 (7)	-0.0856 (6)	0.3416 (4)
C30	0.0055 (8)	-0.0670 (5)	0.3698 (3)
C31	0.0009 (7)	-0.0972 (3)	0.4505 (4)
C32	0.1094 (6)	-0.1429 (4)	0.5042 (3)
C33	0.5862 (6)	-0.1083 (4)	0.5771 (4)
C34	0.1404 (7)	-0.1599 (5)	0.7824 (5)

[a] The form of the anisotropic thermal parameter is as follows: exp[-(B(1,1)*h2 + B(2,2)*k2 + B(3,3)*l2 + B(1,2)*hk + B(1,3)*hl + B(2,3)*ka)]. Estimated standard deviations in the least significant digits are shown in parentheses.

Table II. Carbon–Carbon Bond Lengths (Å) in A_2d

atoms	distance	atoms	distance
C(1)–C(2)	1.401 (7)	C(16)–C(17)	1.601 (8)
C(1)–C(6)	1.399 (7)	C(16)–C(19)	1.591 (8)
C(1)–C(14)	1.504 (8)	C(17)–C(18)	1.490 (8)
C(2)–C(3)	1.396 (9)	C(17)–C(26)	1.594 (8)
C(3)–C(4)	1.365 (9)	C(18)–C(33)	1.554 (8)
C(4)–C(5)	1.376 (8)	C(19)–C(20)	1.534 (8)
C(5)–C(6)	1.356 (8)	C(19)–C(32)	1.515 (8)
C(6)–C(7)	1.543 (7)	C(20)–C(21)	1.384 (8)
C(7)–C(8)	1.524 (8)	C(20)–C(25)	1.383 (7)
C(7)–C(18)	1.565 (8)	C(21)–C(22)	1.369 (9)
C(8)–C(9)	1.391 (8)	C(22)–C(23)	1.377 (9)
C(8)–C(13)	1.399 (7)	C(23)–C(24)	1.388 (8)
C(9)–C(10)	1.363 (8)	C(24)–C(25)	1.377 (8)
C(10)–C(11)	1.372 (8)	C(25)–C(26)	1.499 (8)
C(11)–C(12)	1.363 (8)	C(26)–C(27)	1.520 (8)
C(12)–C(13)	1.371 (7)	C(27)–C(28)	1.375 (8)
C(13)–C(14)	1.512 (7)	C(27)–C(32)	1.406 (7)
C(14)–C(15)	1.541 (8)	C(28)–C(29)	1.391 (10)
C(15)–C(16)	1.505 (8)	C(29)–C(30)	1.361 (10)
C(15)–C(34)	1.539 (8)	C(30)–C(31)	1.378 (9)
		C(31)–C(32)	1.354 (8)

with those reported in the literature.[14,16]

Crude A_2d obtained by allowing A to react thermally with *t*-[4,4]Ad was purified by recrystallization from *n*-hexane. A large ($0.3 \times 0.3 \times 0.3$ mm^3) crystal of A_2d selected from crystals grown by slow evaporation of solvent from the compound was subjected to X-ray structure determination. The Ortep view of the structure shown in Figure 1 confirms Kaupp's assignment.[14] Positional parameters, bond distances, and angles are given in Tables I–III, respectively. Thermal parameters for carbon atoms and positional parameters for hydrogen atoms are available as supplementary material (Tables I-S and II-S, respectively). The numbering system used is shown in the structure.

Table III. CCC Bond Angles (deg) in A_2d

atoms	angle	atoms	angle
C(2)–C(1)–C(6)	119.0 (6)	C(16)–C(17)–C(18)	113.3 (6)
C(2)–C(1)–C(14)	122.0 (6)	C(16)–C(17)–C(26)	108.3 (5)
C(6)–C(1)–C(14)	119.0 (5)	C(18)–C(17)–C(26)	114.3 (5)
C(1)–C(2)–C(3)	119.9 (6)	C(7)–C(18)–C(17)	113.3 (5)
C(2)–C(3)–C(4)	119.4 (6)	C(7)–C(18)–C(33)	110.4 (6)
C(3)–C(4)C(5)	120.4 (6)	C(17)–C(18)–C(33)	110.9 (6)
C(4)–C(5)–C(6)	121.5 (6)	C(16)–C(19)–C(20)	106.8 (5)
C(1)–C(6)–C(5)	119.6 (6)	C(16)–C(19)–C(32)	106.7 (5)
C(1)–C(6)–C(7)	118.3 (5)	C(20)–C(19)–C(32)	107.3 (5)
C(6)–C(7)–C(8)	110.5 (5)	C(19)–C(20)–C(21)	126.1 (6)
C(6)–C(7)–C(18)	114.6 (5)	C(19)–C(20)–C(25)	113.5 (5)
C(8)–C(7)–C(18)	111.6 (5)	C(21)–C(20)–C(25)	120.4 (6)
C(7)–C(8)–C(9)	121.5 (5)	C(20)–C(21)–C(22)	119.7 (6)
C(7)–C(8)–C(13)	118.0 (5)	C(21)–C(22)–C(23)	120.2 (6)
C(9)–C(8)–C(13)	120.5 (5)	C(22)–C(23)–C(24)	120.1 (6)
C(8)–C(9)–C(10)	119.5 (6)	C(23)–C(24)–C(25)	119.9 (6)
C(9)–C(10)–C(11)	120.7 (6)	C(20)–C(25)–C(24)	119.5 (6)
C(10)–C(11)–C(12)	119.6 (6)	C(20)–C(25)–C(26)	113.4 (5)
C(11)–C(12)–C(13)	122.1 (6)	C(24)–C(25)–C(26)	127.1 (6)
C(8)–C(13)–C(12)	117.7 (5)	C(17)–C(26)–C(25)	107.9 (5)
C(8)–C(13)–C(14)	119.8 (5)	C(17)–C(26)–C(27)	106.7 (5)
C(12)–C(13)–C(14)	122.3 (5)	C(25)–C(26)–C(27)	108.7 (5)
C(1)–C(14)–C(13)	109.6 (5)	C(26)–C(27)–C(28)	127.2 (6)
C(1)–C(14)–C(15)	113.1 (5)	C(26)–C(27)–C(32)	111.7 (5)
C(13)–C(14)–C(15)	116.2 (5)	C(28)–C(27)–C(32)	121.1 (6)
C(14)–C(15)–C(16)	112.7 (5)	C(27)–C(28)–C(29)	118.1 (7)
C(14)–C(15)–C(34)	110.1 (5)	C(28)–C(29)–C(30)	121.1 (7)
C(16)–C(15)–C(34)	110.3 (5)	C(29)–C(30)–C(31)	119.8 (7)
C(15)–C(16)–C(17)	113.1 (5)	C(30)–C(31)–C(32)	121.2 (7)
C(15)–C(16)–C(19)	114.9 (5)	C(19)–C(32)–C(27)	114.2 (5)
C(17)–C(16)–C(19)	107.9 (4)	C(19)–C(32)–C(31)	127.1 (6)
		C(27)–C(32)–C(31)	118.6 (6)

(B) Photoreaction Quantum Yields. A loss and photoproduct quantum yields were determined as a function of [D] in benzene. Irradiations were conducted in a Moses merry-go-round apparatus[17] at 30.0 ± 0.1 °C with 366-nm excitation. The benzophenone-sensitized isomerization of *trans*-stilbene was used for actinometry.[18,19] Conversion to *cis*-stilbene corrected for zero-time cis content and back reaction[20] ranged from 1.00 to 16.5%. When necessary, actinometers were irradiated in series with the same A/D samples to avoid larger conversions. Benzophenone and *trans*-stilbene concentrations varied from experiment to experiment but were always close to 0.05 and 0.04 M, respectively. In several experiments irradiation ampules were equipped with Pyrex UV cells attached by side arms. The loss of A was measured by UV spectroscopy immediately following the irradiation period, f_{-A}^0, and at different times during a dark period in which the progress of the thermal addition of *t*-[4,4]Ad to A was followed until no further change in [A] could be detected, f_{-A}^∞. The time required to reach this point was reduced by heating the solutions (60–70 °C) as needed at the end of each kinetics run. Table IV gives representative results. The thermal reaction was also followed conveniently by ^{1}H NMR spectroscopy. Identical kinetics results were obtained by UV in degassed solutions and by NMR in the presence of air. A loss quantum yields, ϕ_{-A}, for degassed and air-saturated solutions are listed in Tables V and VI, respectively.[21] Incident light intensities, I_a (einstein s^{-1}), are also listed for degassed solutions.

The quantum yields for *t*-[4,4]Ad, formation $\phi_{t\text{-}4,4}$, should be greater than or equal to $(\phi_{-A}^\infty - \phi_{-A}^0)$ in Table V. The inequality

(17) Moses, F. G.; Liu, R. S. H.; Monroe, B. M. *Mol. Photochem.* **1969**, *1*, 245.
(18) Hammond, H. A.; DeMeyer, D. E.; Williams, J. L. R. *J. Am. Chem. Soc.* **1969**, *91*, 5180.
(19) Valentine, D., Jr.; Hammond, G. S. *J. Am. Chem. Soc.* **1972**, *94*, 3449.
(20) Saltiel, J.; Marinari, A.; Chang, D. W.-L.; Mitchener, J. C.; Megarity, E. D. *J. Am. Chem. Soc.* **1979**, *101*, 2982.
(21) For more details and additional values at somewhat different concentrations and intensities see: Dabestani, R. Ph.D. Dissertation, The Florida State University, 1985.

Table IV. Dark Time A Loss, 30.0 °C[a]

	f_{-A} (time, h)[b]				
	[D] = 0.174 M	[D] = 0.263 M	[D] = 0.436 M	[D] = 0.872 M	[D] = 1.31 M
	0.293 (0)	0.358 (0)	0.228 (0)	0.233 (0)	0.294 (0)
	0.303 (5.5)	0.369 (5.5)	0.252 (8.3)	0.245 (8.8)	0.312 (8.8)
	0.315 (16.5)	0.382 (16.5)	0.266 (19.2)	0.263 (19.8)	0.330 (19.8)
	0.321 (24.5)	0.391 (24.5)	0.270 (27.2)	0.270 (27.8)	0.342 (27.8)
	0.337 (40.8)	0.409 (40.8)	0.284 (43.4)	0.277 (44.0)	0.362 (44.0)
	0.344 (47.4)	0.418 (47.4)	0.298 (50.4)	0.293 (51.1)	0.374 (51.1)
	0.369 (93.9)	0.456 (93.9)	0.318 (96.2)	0.314 (96.8)	0.405 (96.8)
	0.418 (163)	0.507 (163)	0.372 (165)	0.382 (166)	0.472 (166)
hot[c]	0.425	0.529	0.380	0.389	0.499

[a] $[A]_0 = 2.75 \times 10^{-3}$ M, throughout; see Table IV for corresponding ϕ_{-A}^0 values. [b] Solutions monitored by UV after irradiation period, $t = 0$, and following dark periods at 30.0 °C with the UV cell ($l \sim 0.09$ cm) attached to ampule (no sample handling). [c] Solutions heated 2 h at 60–70 °C prior to final measurement.

Table V. Anthracene Loss Quantum Yields, Degassed Solutions

[D], M	$[A]_0 \times 10^3$, M	$[\bar{A}] \times 10^3$, M	ϕ_{-A}[a]	ϕ_{-A}^∞	$I_a \times 10^9$, einstein/s
0	8.3_0	7.3_9	0.100		
0.065_4	8.3_4	7.7_8	0.101 (3)		
0.174	8.2_0	7.3_3	0.141	0.211	1.13
0.263	8.4_0	7.6_9	0.158 (4)	0.22_8	1.13
0.43_6	8.2_5	7.2_2	0.202	0.33_1	1.13
	8.3_5	7.5	0.196 (13)		
0.87_2	8.70	7.6_4	0.242	0.42_2	1.06
	8.3_5	7.5	0.235 (5)		
1.31	8.5_7	7.3_2	0.286	0.49_3	1.68
	8.3_0		0.264 (18)		
0.174	2.76	2.36	0.102	0.148	1.20
0.263	2.73	2.24	0.123	0.182	1.20
0.43_6	2.77	2.45	0.158	0.26_3	1.21
0.87_2	2.74	2.42	0.218	0.36_4	1.22
1.31_8	2.74	2.34	0.276	0.46_8	1.22
0.052_4	0.60_5	0.54_9	0.0403 (8)	0.054_2	1.18
0.087_2	0.60_3	0.52_9	0.0537 (6)	0.075_5	1.18
0.131	0.59_8	0.55_1	0.077_7		1.12
0.140	0.60_4	0.51_0	0.0817 (10)	0.119	1.12
0.174	0.60_5	0.55_1	0.0858 (14)	0.131	1.08
	0.60_6	0.53_8	0.089_8	0.136	1.18
	0.61_4	0.54_4	0.0920 (10)	0.135	5.17
0.263	0.60_6	0.51_7	0.117	0.181	1.18
0.43_6	0.60_6	0.50_9	0.16_0	0.24_8	1.22
0.87_2	0.60_6	0.50_1	0.23_7	0.37_8	1.18
	0.60_6	0.51_7	0.21_3	0.38_3	1.14
1.31	0.60_6	0.52_1	0.28_4	0.52_5	1.11

[a] Values in parentheses are uncertainties in the last decimal places from multiple determinations; all analyses by UV.

stems from the fact that at the higher [A] values and low I_a's, ϕ_{-A}^0 includes some A loss due to the thermal reaction of *t*-[4,4]Ad with A during the course of the irradiation. To avoid this uncertainty and to obtain accurate dimerization quantum yields, ϕ_{A_2}, a series of experiments was carried out with A-^{14}C in degassed benzene. Following complete conversion of *t*-[4,4]Ad to A_2d, yields of A_2d and A_2 were determined by isotopic dilution (see Experimental Section), Table VII. Since f_{-A}^0 and f_{-A}^∞ values were also measured as described in the previous paragraph, an independent set of ϕ_{-A}^0 and ϕ_{-A}^∞ values is included in Table VII. The table also lists results for solutions in which azulene, Az, or methyl iodide, MeI, is included.

Quantum yields for [2,4]Ad, $\phi_{2,4}$, and an unidentified minor peak, ϕ_x, were based on GLC analysis with use of *trans*-stilbene or benzophenone as internal standards. Since erratic results were obtained from solutions containing *t*-[4,4]Ad, GLC analyses were carried out after the completion of thermal formation of A_2d. The minor adduct peak is absent in the presence of air or azulene ($\phi_x = 0$) and barely discernible when $[A]_0 \simeq 8 \times 10^{-3}$ M. Additional minor peaks were noted in the presence of air ($\phi < 10^{-3}$) but are not included since their identity was not investigated. Since these were mostly independent experiments, they resulted in additional ϕ_{-A} values. Quantum yields obtained as a function of [D] at two different concentrations of A are given in Table VIII. Table IX gives data in the presence of Az and MeI.

Table VI. Anthracene Loss Quantum Yields in the Presence of Air

[D], M	$[A]_0 \times 10^3$, M	$[\bar{A}] \times 10^3$, M	ϕ_{-A}	$(\phi_{Ad})_{air} \times 10^2$[a]
0.174	8.3_3	6.7_4	0.108	3.14
0.263	8.3_7	6.5_7	0.123	5.04
0.43_6	8.2_9	6.7_6	0.148	7.79
0.87_2	8.4_5	6.8_8	0.188	12.6
1.31	8.2_7	6.1_0	0.26_0	21.0
0.174	2.71	2.51	0.073_3	4.13
0.263	2.70	2.45	0.092_8	6.26
0.43_6	2.74	2.46	0.128	9.96
0.87_2	2.72	2.44	0.195	17.1
1.31	2.71	2.37	0.23_7	21.6
0.052_4	0.59_8	0.55_5	0.022_4	1.45
0.087_2	0.59_8	0.53_9	0.030_6	2.30
0.131	0.59_8	0.54_6	0.041_2	3.37
0.140	0.60_2	0.54_5	0.040_0	3.39
0.175	0.59_6	0.54_5	0.050_8	4.47
0.217	0.59_8	0.53_9	0.061_7	5.45
0.263	0.59_6	0.52_7	0.068_3	6.40
0.43_6	0.59_8	0.51_2	0.110	10.8
0.87_2	0.58_2	0.47_3	0.174	17.6
1.31	0.58_6	0.43_5	0.23_8	24.3

[a] Calculated by using eq 10 and 11, see text.

The role of triplets in the A/D system was investigated with fluorenone as the triplet energy donor in benzene. The conditions and procedures described above were employed except that 404- and 436-nm Hg lines were used for excitation and the fluorenone-sensitized isomerization of *trans*-stilbene was used for actinometry.[19,22] Concentrations of fluorenone (7.0×10^{-3} or 5.0×10^{-3} M) were matched in actinometer and A/D solutions. Quantum yields for A loss (UV) and adduct formation (GLC), $\phi_{2,4}$ and ϕ_x, are given in Table X. Also given in Table X are ϕ_{-A} and $\phi_{t\text{-}4,4}$ values obtained by isotopic dilution with A-^{14}C. Quantum yields for the trans–cis fluorenone sensitized isomerization of the diene (GLC) in the presence of A were measured for two diene concentrations (Table XI).

(C) Fluorescence Measurements. The effect of azulene, $0 \leq [Az] \leq 5.2 \times 10^{-5}$ M, on A fluorescence, $[A] = 1.13 \times 10^{-4}$ M, $\lambda_{exc} = 349$ nm, was examined in air-saturated benzene. No effect was observed within the uncertainty of these measurements, ±7% (Table III-S). On the other hand, significant quenching of A fluorescence by MeI was observed in air-saturated benzene, $[A] = 1.12 \times 10^{-4}$ M, $\lambda_{exc} = 349$ nm, 23 °C. No effect on A absorbance by MeI was noted in the UV spectra of these solutions. Results obtained by averaging I_0/I values for the fluorescence maxima at $\lambda = 385$, 400, and 420 nm are given in Table XII.

Discussion

In a series of papers starting in 1968 Liu and co-workers showed that a higher triplet state of anthracenes, T_2 (in several anthracenes T_2 is 68–74 kcal/mol and T_1 is 40–42.5 kcal/mol above S_0),

(22) Caldwell, R. A.; Gajewski, R. P. *J. Am. Chem. Soc.* **1971**, *93*, 532.
(23) Saltiel, J.; Metts, L.; Wrighton, M. *J. Am. Chem. Soc.* **1971**, *93*, 5302.

Table VII. Product Quantum Yields by Isotopic Dilution[a]

[D], M	$[A]_0 \times 10^3$, M	$[\bar{A}] \times 10^3$, M	ϕ_{-A}	$\phi_{A_2} \times 10^2$	$\phi_{t\text{-}4,4} \times 10^2$ [b]	$I_a \times 10^9$, einstein/s
0.26_3	8.3_4	7.4_8	0.130	3.5_6	4.6_6 (3.2)	5.52
0.26_3	8.4_0	7.7_1	0.15_5	4.64 (9)	$4.5_2 \pm 0.04$	1.11
0.43_6	8.3_2	7.3_5	0.18_3	3.8_8	9.0_1 (6.1)	6.00
0.43_6	8.4_0	7.4_8	0.17_9	4.38 (8)	8.3 ± 0.3	1.13
0.87_2	8.4_0	7.5_2	0.23_6	3.4_7	13.3	1.70
0.26_3	1.91	1.7_5	0.102	1.11	6.8_7 (4.6)	1.43
0.174	0.61_4	0.54_4	0.093_1	0.84_5	3.9_8 (3.7)	5.32
0.26_3	0.61_0	0.50_5	0.115	0.55_1 (0)	5.90 ± 0.08 (5.8)	1.37
0.26_3	0.60_0	0.52_2	0.128	0.584 (6)	5.55 ± 0.05	0.935
0.26_3	0.60_8	0.50_8	0.108	0.684 (22)	4.86 ± 0.14	6.18
0.43_6	0.61_3	0.53_3	0.19_0	0.65_9	11.1 (9.9)	4.21
0.26_3	0.63_7	0.57_3	0.110	0.61_8	5.05 (4.5)	3.94
0.26_3[c]	0.63_7	0.56_4	0.072_7	0.52_3	4.98 (5.0)	4.09
0.26_3[d]	0.63_7	0.56_8	0.071_9	0.59_2	5.0_0 (5.1)	4.09
0.26_3[e]	0.63_7	0.55_5	0.065_7	0.37_9	4.8_6 (5.1)	4.09
0.86_2[f]	0.60_2	0.49_0	0.118	0.30_6	0.55_2 (0.55)	3.30
0.87_2[g]	0.61_2	0.51_7	0.099_1	0.21_5	0.27_6 (0.48)	3.30

[a] Loss of A by UV. [b] Values in parentheses from A loss due to thermal reaction with Ad following irradiation, UV; ranges are deviations from mean for duplicate analyses. [c] $[Az] = 2.20 \times 10^{-5}$ M. [d] $[Az] = 3.30 \times 10^{-5}$ M. [e] $[Az] = 4.40 \times 10^{-5}$ M. [f] [MeI] = 0.632 M. [g] [MeI] = 1.28 M.

Table VIII. Quantum Yields for Minor Adducts by GLC[a]

[D], M	$[A]_0 \times 10^3$, M	ϕ_{-A}[b]	$\phi_{2,4} \times 10^3$	$\phi_x \times 10^3$	$I_a \times 10^9$, einstein/s
0.043_6	0.61_1		(1.8)		
0.052_4	0.59_8	0.046_1 (0.022_4)	9.9 (2.0)	1.3[c]	1.62
	0.63_0	0.044_6	9.7	2.9	1.62
0.065_4	0.61_1		(2.7)		
0.087_2	0.59_8	0.064_9 (0.030_6)	15.0 (4.1)	2.1[c]	1.62
	0.63_0	0.060_7	14.7	4.4	1.62
0.131	0.59_8	0.077_6 (0.041_1)	$21._2$ (4.7)	3.2[c]	1.62
0.140	0.63_0	0.082_0	$22._7$	6.2	1.62
0.174	0.59_8	0.105 (0.051_5)	$26._2$ (7.9)	3.5[c]	1.62
	0.63_0	0.110	$24._6$		1.62
0.217	0.59_8	0.120	$29._3$ (9.1)	4.2[c]	1.62
0.26_3	0.60_0	0.128	$40._3$ ($11._2$)	9.7	0.94
	0.61_1		$32._1$	4.0[c]	0.90
	0.63_7	0.111	$46._8$	9.1	4.09
0.43_6	0.61_1		$55._3$ ($14._2$)		0.90
0.61_6	0.61_1		$63._7$ ($19._0$)		0.90
0.87_2	0.59_2	0.234	$56._2$	13.1	2.98
1.31	0.61_1		(33)		
1.74	0.61_1		(24)		
0.065_4	8.3_4	0.089	2.1_6		1.46
0.174	8.3_0	0.130	4.6_0		1.64
	8.3_0	0.134	4.9_4		1.64
0.26_3	8.4_0	0.155	7.3_7		1.64
0.43_6	8.4_0	0.18_4	10.8		1.64
0.87_2	8.4_0	0.23_7	$15._7$		1.64
1.31	8.3_4	0.25_0	$21._0$		1.46

[a] Values in parentheses are for air-saturated solutions. [b] By UV; values obtained by GLC were always higher due to A_2d formation during workup; values for high [A] (last seven rows) estimated to be 5% high due to thermal A_2d formation during the course of the irradiation (17 h); conversions, $f_{-A}^0 \leq 0.20$. [c] GLC procedure 1, under these conditions a second longer retention time peak was obtained ($\phi_x' \times 10^4 = 2.0, 3.5, 4.6, 4.2, 5.4$ in order given in column); other entires in this column are for GLC procedure 2.

Table IX. The Effects of Azulene and Methyl Iodide on Quantum Yields[a]

$[A]_0 \times 10^4$, M	$[Az] \times 10^5$, M	[MeI], M	ϕ_{-A}^0[b]	$\phi_{A_2} \times 10^3$[c]	$\phi_{t\text{-}4,4} \times 10^2$[c,d]	$\phi_{2,4} \times 10^2$[e]	$\phi_x \times 10^2$[e]
6.3_7	0	0	0.104	7.1_6	5.8_5[f] (5.4)	4.4_3	0.83
6.3_7	0	0	0.110		(4.5)	4.9_4	0.98
6.37	1.1_0	0	0.075_1		(4.5)		
6.3_7	2.1_8	0	0.077_9	6.0_6	5.7_3 (5.8)	1.2_4	0
6.3	3.2_8	0	0.077_4	6.8_6	5.7_9 (5.9)		
6.3_7	4.3_7	0	0.076_8	4.3_9	5.6_3 (5.9)	0.95	0
6.3_7	5.5_0	0	0.075_6		(5.3)	1.0_7	0
5.9_2	0	0	0.23_4		(13.2)	5.1	1.1_8
5.9_2	0	0.161	0.176		(1.7)	9.8	2.7
5.9_2	0	0.32_1	0.151		(2.2)	9.6	2.6
6.0_2[g]	0	0.64_2	0.118	3.0_6	0.55_2 (0.56)	9.5	1.9
6.1_2	0	1.28	0.099_1	2.1_5	0.27_6 (0.48)	7.4	1.7

[a] Az experiments rows 1–7, [D] = 0.263 M, $I_a \simeq 4.0 \times 10^{-9}$ einstein/s. MeI experiments rows 8–12, [D] = 0.87_2 M, except as noted, $I_a \simeq 3.0 \times 10^{-9}$ einstein/s. [b] UV. [c] Scintillation counting. [d] Values in parentheses $\phi_{-A}^\infty - \phi_{-A}^0$, by UV. [e] GLC procedure 2. [f] Assumed and used as actinometer for Az experiments. [g] [D] = 0.85_8 M.

Table X. Quantum Yields for Fluorenone-Sensitized Dimer and Adduct Formation[a]

$[A]_0 \times 10^3$, M	[D], M	$\phi_{-A} \times 10^2$	$\phi_{A_2} \times 10^3$	$\phi_{t\text{-}4,4} \times 10^4$	$\phi_{2,4} \times 10^3$	$\phi_x \times 10^3$	$I_a \times 10^8$,[b] einstein/s
0.62	0	1.8_6	9.3[c]				4.8
3.62	0	0.38	1.9[c]				6.2
8.33	0	0.18	0.9[c]				6.0
2.71	0.140	1.7_3			9.4	2.5	5.1
2.64	0.174	1.8_7			$13._8$	4.5	1.7
2.64	0.26_3	2.3_7			$18._5$	5.7	1.7
2.64	0.43_6	3.1_7			$24._8$	$8._3$	1.7
2.71	0.87_2	3.9_1			$29._1$	$8._2$	1.7
1.81	0.26_3	2.5	2.4		13.1	5.1	7.0
1.87	0.26_3	1.81	1.4	3			3.2
1.87	0.26_3	1.9_4	1.8	2			8.6
1.87	0.43_6	2.2_7	1.0	6			3.0
1.87	0.43_6	2.1_5	1.2	3			7.8

[a] Fluorenone concentration 7.0×10^{-3} M, except four last rows for which it was 5.0×10^{-3} M; A loss by UV; ϕ_{A_2} and $\phi_{t\text{-}4,4}$ by isotopic dilution starting with A-^{14}C unless otherwise noted; $\phi_{2,4}$ and ϕ_x by GLC, procedure 2. [b] Corresponds to photons absorbed at 404 and 436 nm; light incident on the solutions was 55% higher than these values for [Fl] = 5×10^{-3} M. [c] $\phi_{A_2} = (1/2)\phi_{-A}$.

Table XI. Fluorenone-Sensitized Trans–Cis Photoisomerization of D[a]

[D], M	[A] $\times 10^3$, M	$\phi_{tt \rightarrow ct}$	ref
0.174	0	0.33	23
0.140	2.71	0.070	this work
0.87_2	2.71	0.23	this work

[a] [F] = 7.0×10^{-3} M; no cis,cis isomer was detected in the presence of A.

Table XII. The Effect of MeI on A Fluorescence, 23 °C[a]

[MeI], M	I_0/I	[MeI], M	I_0/I
0	1	0.40_4	7.61 ± 0.21
0.081	2.13 ± 0.03	0.80_8	17.2 ± 0.3
0.161	3.12 ± 0.08	1.21_2	24.5 ± 2.0

[a] [A] = 1.12×10^{-4} M in air-saturated benzene; λ_{exc} = 349 nm; uncertainties are average deviations from the mean of relative intensities for emission maxima at 385, 400, and 420 nm.

functions as a donor of triplet excitation to a variety of acceptors.[24] A strong case for T_2 sensitization was made with structurally rigid acceptors having relatively high lowest triplet excitation energies (62–69 kcal/mol), but results with flexible acceptors such as the 1,3-pentadienes[24d] and the stilbenes[24c,e] were open to alternative interpretation. The lowest triplet energies of these flexible acceptors (*s-cis*-diene ~52 kcal/mol, stilbene ~49 kcal/mol)[25] could also be reached by endothermic energy transfer from the much longer lived T_1 state of anthracene. About 15 years ago we began a research program whose aim was the resolution of this T_2 vs. T_1 ambiguity. Both anthracene and 9,10-dichloroanthracene sensitization of stilbene triplet formation was indeed shown to involve T_1 excitation transfer exclusively.[26,27] In resolving the question of the mechanism of diene triplet formation we examined the anthracene-sensitized trans–cis photoisomerization of *trans,trans*-2,4-hexadiene. Liu's mechanism of T_2 sensitization was confirmed for this diene by utilizing the striking decay fraction difference of s-trans and s-cis triplets and the high sensitivity on the energy of the triplet donor of relative populations of these triplets.[23] The large A losses noted during the course of this research led to the proposal of the exciplex mediated mechanism for A dimerization (eq 3)[7] and to the investigation of other aspects of A and A/D photophysics and photochemistry.[4,5,28,29] This previous work provides the foundation on which the mechanism for photocycloaddition in the A/D system must be based.

(A) Cycloadducts. The structures of the three cross-adducts *t*-[4,4]Ad, *c*-[4,4]Ad, and [2,4]Ad have been based primarily on ^{1}H NMR spectra[14,16] which were confirmed in this work. In addition, Yang showed that reduction of the double bond in the two [4 + 4] adducts gives the same dihydro derivative and that *t*-[4,4]Ad can be converted to *c*-[4,4]Ad by xanthone-sensitized photoisomerization.[16] The latter observation could not be reproduced by Kaupp[14] but was readily reproduced in this work. GLC analyses of reaction mixtures before and after the xanthone-sensitized reaction established that *t*-[4,4]Ad did not contribute to the chromatogram while *c*-[4,4]Ad gave a peak with a significantly longer retention time than the peak corresponding to [2,4]Ad. The yield of [2,4]Ad is enhanced when MeI is included in direct excitation experiments and is diminished when the triplet quenchers Az or O_2 are included. Its formation by both singlet and triplet pathways is supported by the fact that it becomes the major product when fluorenone is employed as a triplet sensitizer. Little or no *t*-[4,4]Ad forms upon triplet sensitization and no *c*-[4,4]Ad is detected in GLC traces or ^{1}H NMR spectra of reaction mixtures under these conditions. Formation of *c*-[4,4]Ad was detected in ^{1}H NMR spectra of reactions carried out to complete A loss under direct excitation conditions. It may have been one of several minor peaks in GLC traces which were considered too small for accurate quantum yield determinations. Of the minor peaks only one (retention time between [2,4]Ad and *c*-[4,4]Ad) was considered of mechanistic significance because it comprised about 30% of adduct area in chromatograms from sensitized reactions and the MeI and triplet quenching experiments showed it to arise solely from triplet precursors. It was not isolated and its structure is unknown, though the cis isomer of [2,4]Ad (methyl cis to vinyl substituent on the bridge) is a likely candidate. It is the product x-Ad in the Results section which, as will be shown below, affords an excellent criterion for the relative importance of the triplet pathway to adducts as reactant concentrations are varied. In those instances where A loss and all major product yields were measured, excellent mass balance was achieved as reflected in the relationship $\phi_{-A} \simeq (2\phi_{A_2} + \phi_{t\text{-Ad}} + \phi_{2,4} + \phi_x)$.

Finally, the NMR spectra of reaction mixtures established that A_2d is probably not a photoproduct but arises from thermal reaction of A with *t*-[4,4]Ad as proposed by Kaupp.[14] This compound was isolated in crystalline form and its structure was established by X-ray crystallography (Figure 1). Since the trans relationship of the double bond in *t*-[4,4]Ad is reflected in A_2d, the structure of *t*-[4,4]Ad is confirmed by inference as is that of *c*-[4,4]Ad.

In the following sections it will be shown that Scheme I, which summarizes the known chemistry of the A/D system, accounts quantitatively for the cycloaddition results.

(24) (a) Liu, R. S. H.; Edman, J. R. *J. Am. Chem. Soc.* **1968**, *90*, 213. (b) Liu, R. S. H.; Gale, D. M. *Ibid.* **1968**, *90*, 1897. (c) Liu, R. S. H. *Ibid.* **1968**, *90*, 1899. (d) Liu, R. S. H.; Edman, J. R. *Ibid.* **1969**, *91*, 1492. (e) Lau, K. S. Y.; Campbell, R. O.; Liu, R. S. H. *Mol. Photochem.* **1972**, *4*, 315. (f) Campbell, R. O.; Liu, R. S. H. *J. Am. Chem. Soc.* **1973**, *95*, 6560.

(25) Saltiel, J.; Charlton, J. L. *Rearrangements in Ground and Excited States*; de Mayo, P., Ed.; Academic Press: New York, 1980; Vol. 3, p 25 and references cited.

(26) Saltiel, J.; Marchand, G. R.; Kirkor-Kaminska, E.; Smothers, W. K.; Mueller, W. B.; Charlton, J. L. *J. Am. Chem. Soc.* **1984**, *106*, 3144.

(27) Saltiel, J.; Townsend, D. E.; Sykes, A. *J. Am. Chem. Soc.* **1983**, *105*, 2530.

(28) Watson, B. D.; Townsend, D. E.; Saltiel, J. *Chem. Phys. Lett.* **1976**, *43*, 295.

(29) Saltiel, J.; Marchand, G. R.; Dabestani, R.; Pecha, J. M. *Chem. Phys. Lett.* **1983**, *100*, 219.

Scheme I

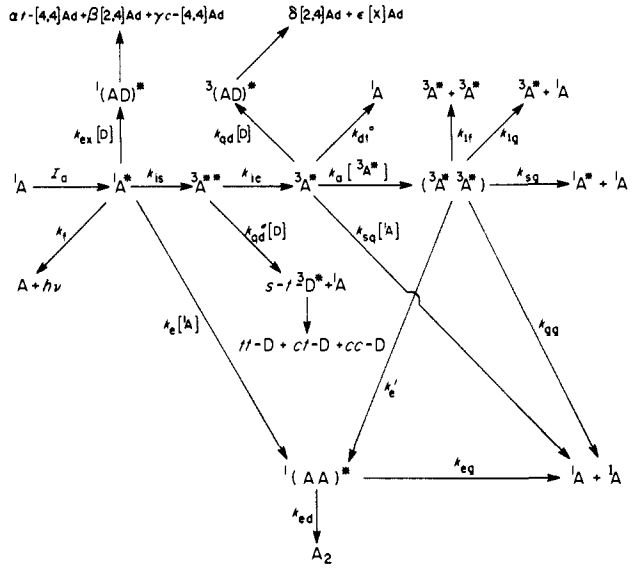

Table XIII. Rate Constants for A_2d Formation in Benzene[a]

[A] × 10³,[b] M	T, °C	k × 10³, M⁻¹ s⁻¹	method
0.61	30.0	1.1 (1)	UV
	52.0	14 (3)	UV
2.8	30.0	1.2 (2)	UV
8.5	30.0	1.09 (3)	UV
85.0[c]	30.0	0.90	NMR

[a] Unless otherwise indicated, separate runs were carried out for [D] = 0.174, 0.263, 0.436, 0.872, and 1.31 M for each [A]. [b] $[A]_0$ for thermal reaction ~20–30% less than indicated values and $[t\text{-}[4,4]Ad]_0 \sim 0.2[A]_0$. [c] [D] = 0.32 M.

(B) Thermal Diels–Alder Reaction of *t*-[4,4]Ad with A. The reaction of A with *t*-[4,4]Ad was conveniently followed in the original degassed solutions with use of a UV cell of appropriate path length (0.2–2 mm) attached to the irradiation ampule by a side arm. The results shown in Table IV are typical. Similar results were obtained for the diene concentrations listed in Table IV for $[A]_0 \simeq 8.5 \times 10^{-3}$ M and with $[A]_0 = 6.1 \times 10^{-4}$ M at 30 °C. Since the progress of the reaction for solutions with $[A]_0 \simeq 6 \times 10^{-4}$ M was slow (about 25% conversion to A_2d after 85.5 h at 30 °C), the bath temperature was increased to 52 °C and kinetics measurements were continued for ~100 h. The reactions were also followed in the presence of air by ^1H NMR spectroscopy at 30 °C starting with $[A] = 8.5 \times 10^{-2}$ M and [D] = 0.32 M. There was generally good adherence to the second-order rate law[30]

$$\frac{1}{a_0 - b_0} \ln \frac{a_0 b}{b_0 a} = kt \qquad (4)$$

where *a* and *b* represent [A] and [*t*-[4,4]Ad], respectively. The rate constants, summarized in Table XIII, are independent of initial reactant concentrations or of the presence of large D concentrations. The conversion of *t*-[4,4]Ad to A_2d is therefore quantitative. The temperature effect on *k* allows a rough estimation of Arrhenius parameters: $E_a = 22.6 \pm 3$ kcal/mol and $\log A = 13.37 \pm 1$. The quantum yields for A loss corresponding to these kinetics runs, shown in Table V (ϕ_{-A}^0 for initial A loss and ϕ_{-A}^∞ for A loss after the completion of the thermal reaction), qualitatively account for the large values we reported previously.[7] In that work, $[A]_0 = 8.3 \times 10^{-3}$ M was employed and duplicate solutions were analyzed by GLC after concentration on a hot plate or by UV 2 weeks following the irradiation. In both cases the thermal reaction was complete and the reported quantum yields corresponded to ϕ_{-A}^∞. The differences ($\phi_{-A}^\infty - \phi_{-A}^0$) from Table V are close to independently measured $\phi_{t\text{-}4,4}$ values (see below).

(30) Frost, A. A.; Pearson, R. G. *Kinetics and Mechanism*, 2nd ed.; Wiley: New York, 1961; p 16.

Table XIV. Parameters Used in Computing Quantum Yields[a]

parameter	value	ref
p_t	1.40	5, 35
p_s	0.046	5, 35
p_{ed}	0.22	5, 12
p_e'	0.115	5
k_a	9.6×10^9 M⁻¹ s⁻¹	5, 12, 36
k_e	9.6×10^9 M⁻¹ s⁻¹	5, 12
k_f	6.43×10^7 s⁻¹	5, 37
k_{is}	1.74×10^8 s⁻¹	5, 38
τ_m^0	4.2×10^{-9} s	5, 37
k_{dt}^0	49 s⁻¹	5, 29
k_{sq}	3.73×10^5 M⁻¹ s⁻¹	5, 29
$k_{ex}\tau_m^0$	0.57	28
k_{qd}'/k_{ic}	0.26	27
k_{qd}	1×10^3 M⁻¹ s⁻¹	27
$k_{qs}[O_2]$	4.5×10^7 M⁻¹ s⁻¹	5, 12
$k_{qt}[O_2]$	5.6×10^6 M⁻¹ s⁻¹	5, 35
α	0.46 ± 0.02	(calcd)
β	0.08 ± 0.02	(calcd)
γ	0.02_5 ± 0.01	(calcd)
δ	0.133 ± 0.02	(calcd)
ϵ	0.04_7 ± 0.01	(calcd)

[a] See footnotes for Table II in ref 5.

(C) Photocycloaddition Reactions. In the absence of diene Scheme I reduces to the one used to account quantitatively for the intensity and concentration dependencies of A photodimerization quantum yields.[5] ($^3A^*{}^3A^*$) represents the two triplet encounter pair, and the remaining terms are self-explanatory. Literature sources of all rate constants are given in Table XIV. When D is introduced in the solution it interacts with a minimum of three A excited states, the lowest excited singlet state, $^1A^*$, the initially formed higher excited triplet state, $^3A^{**}$, and the lowest triplet state $^3A^*$. The rate constant for the first of these processes is known from fluorescence quenching measurements (steady state and transient)[28] and the rate parameters for the interactions of D with A triplets are available from our study of the A-sensitized trans–cis photoisomerization of D.[27] The singlet excimer and exciplex intermediates are included since they have been observed to fluoresce weakly.[28,31,32] Though the quenching rate constant of $^3A^*$ by D is available from a flash kinetic spectroscopic study and from the effect of [D] on the $^3A^*$ sensitized photoisomerization of *trans*-stilbene,[27] there is no direct evidence for the triplet exciplex intermediate shown tentatively in Scheme I. The $^3A^*/D$ interaction could lead directly to a triplet biradical as the key intermediate to cross-adducts. Notable omissions from Scheme I are termolecular interactions of the type shown in eq 2 and 3. It will be shown below that our data are explained well by Scheme I and that eq 2 and 3 do not contribute to the photochemistry. We will consider the effect of [D] on A_2 formation first and after that the singlet and triplet pathways to formation of cross-adducts.

(a) Anthracene Dimerization. A full exposition of the kinetics for anthracene photodimerization is given in the Appendix of ref 5. The steady-state solution for ϕ_{A_2} is

$$\phi_{A_2} = \frac{p_{ed}}{I_a}\left[\frac{I_a k_e[^1A]}{C} + \left(\frac{p_s k_e[^1A]}{C} + p_e'\right)k_a[^3A^*]_{ss}\right]^2 \qquad (5)$$

where $p_{ed} = k_{ed}/(k_{ed} + k_{eg})$, $p_s = k_{sg}/G$, $p_e' = k_e'/G$, $C = (k_{is} + k_f + k_e[^1A] + k_{ex}[^1D])$, $G = (k_{tt} + k_{tg} + k_{sg} + k_{gg} + k_e')$, and $[^3A^*]_{ss}$, the steady-state triplet concentration, is given by

$$[^3A^*]_{ss} = \frac{k_{dt} - \left[k_{dt}^2 - 4k_a\left(-2 + p_t + \frac{p_s f_{ic} k_{is}}{C}\right)\frac{f_{ic} k_{is} I_a}{C}\right]^{1/2}}{2k_a\left(-2 + p_t + \frac{p_s f_{ic} k_{is}}{C}\right)} \qquad (6)$$

(31) Vember, T.; Veselova, T. V.; Abyknovennaya, I. E.; Cherkasov, A.; Shirokov, V. *Izv. Akad. Nauk SSSR, Ser. Fiz.* **1973**, *37*, 837.

(32) McVey, J. K.; Shold, D. M.; Yang, N. C. *J. Chem. Phys.* **1976**, *65*, 3375.

Table XV. The Effect of [D] on Dimerization Quantum Yields

$[A]_0 \times 10^3$, M	[D], M	obsd[a] $\phi_{A_2} \times 10^2$	calcd[b] $\phi_{A_2}{}^S \times 10^2$	calcd[b] $\phi_{A_2}{}^T \times 10^2$	calcd[b] $\phi_{A_2} \times 10^2$	I_a,[a] einstein s^{-1}
0.61_4	0.174	0.84	0.43	0.32	0.75	5.3
0.60_8	0.263	0.68	0.39	0.24	0.63	6.2
0.61_3	0.43_6	0.66	0.37	0.10	0.47	4.2
8.4_0	0.263	4.6_4	4.4_5	0.015	4.4_7	1.1
8.4_0	0.43_6	4.3_8	4.0_7	0.012	4.0_8	1.1
8.4_0	0.87_2	3.4_7	3.5_4	0.012	3.5_5	1.7

[a] From Table VII. [b] Predicted by eq 5 and 6: first column $^1A^*$ contribution, second column TTA contribution, third column total yield.

where $p_t = (2k_{tt} + k_{tg})/G$, $f_{ic} = k_{ic}/(k_{ic} + k_{qd'}[D])$, and $k_{dt} = (k_{dt}{}^0 + k_{sq}[^1A] + k_{qd}[^1D])$. Modifications required by the presence of D were addition of known terms $k_{ex}[^1D]$ and $k_{qd}[^1D]$ in C and k_{dt}, respectively, and inclusion of the known f_{ic} factor. As defined, f_{ic} varies between 0.99 and 0.75 for the range of [D] employed. It surely overestimates the effect of [D] on the efficiency of $^3A^{**} \rightarrow {}^3A^*$ internal conversion because it neglects the likely back transfer of triplet energy from *s-t*-$^3D^*$ to the geminate ^1A partner.

$$(s\text{-}t\text{-}{}^3D^*{}^1A) \rightarrow tt\text{-}D + ct\text{-}D + cc\text{-}D + {}^3A^* \qquad (7)$$

If the relaxation of the diene triplet in the solvent cage is fast such transfer could occur without substantially changing the cis/trans decay fractions.[33] Since the rate constant for triplet excitation transfer from 2,5-dimethyl-2,4-hexadiene triplets to A has been shown to be close to half the diffusion-controlled limit,[34] $f_{ic} \simeq 1$ is assumed in this section (cf. also eq 12 below).

As can be seen by examining eq 5 and 6 and Table XIV, literature values are available for all parameters needed to calculate ϕ_{A_2} as a function of $[\overline{^1A}]$, $[^1D]$, and I_a. For the calculations it was assumed that the path length was 1.33 or 1.08 cm (depending on ampule size: 1.5 or 1.3 cm o.d.) and that light intensity was uniform over the entire irradiated area (1.34 cm^2). Light absorption decreases exponentially with depth over the exposed portion of the solution. Absorbed light and yield of dimer were calculated for small increments of the solution and summed to obtain the effective quantum yields employing computer assistance; see Appendix, ref 5. Selected ϕ_{A_2} values from Table VII are compared to calculated ϕ_{A_2} values in Table XV. The observed decrease in ϕ_{A_2} as [D] is decreased is reproduced well especially at the higher anthracene concentrations where dimerization accounts for 30–60% of A loss (compare $2\phi_{A_2}$ with ϕ_{-A} in Table VII). Calculated singlet and TTA contributions, $\phi_{A_2}{}^S$ and $\phi_{A_2}{}^T$, respectively, are shown separately in Table XV. As expected $\phi_{A_2}{}^T$ is very sensitive to the magnitude of k_{dt} in eq 6. At low $[^1A]$ the observed effect of $[^1D]$ on ϕ_{A_2} is thus expected to reflect mainly a large decrease in $\phi_{A_2}{}^T$ arising from the $k_{qd}[^1D]$ term in k_{dt}. At high $[^1A]$ the $\phi_{A_2}{}^T$ contribution becomes negligible (~0.3% of total) because of the self-quenching of $^3A^*$ (the $k_{sq}[^1A]$ term in k_{dt}), and the decrease in ϕ_{A_2} reflects mainly the effect of [D] on $\phi_{A_2}{}^S$. We conclude that Scheme I quantitatively accounts for the effect of [D] on ϕ_{A_2} and that Kaupp's claim[14] that the exciplex (the excimer is known to be much too short-lived, 1.5 ns,[32,39] to have been intercepted by D) does not provide a pathway to A_2 has been confirmed.

(b) The Singlet Pathway to Cross-Adducts. Formation of arene/diene exciplexes was suggested to account for the quenching

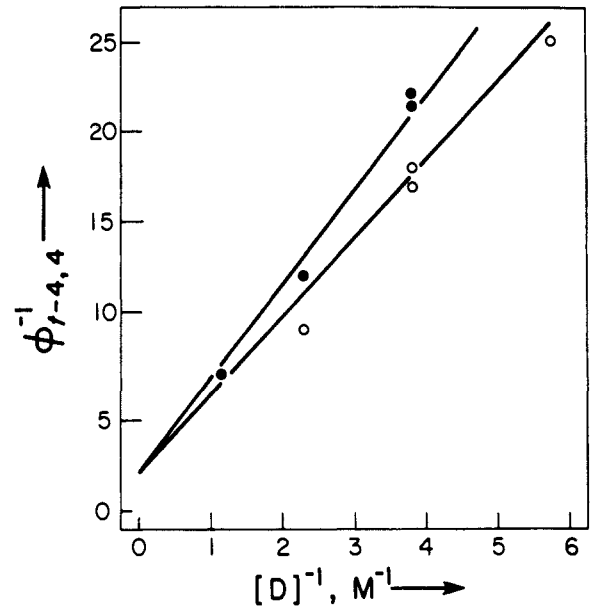

Figure 2. Diene concentration dependence of $\phi_{t\text{-}4,4}$ at high (●) and low (○) anthracene concentration (eq 8).

of arene fluorescence by 1,3-dienes[40] and later confirmed in specific cases by the observation of exciplex fluorescence.[7,12,41,42] Compelling evidence for the collapse of singlet exciplexes to cycloadducts[41b,42,43] was reported for phenanthrene/olefin systems where identical quenching efficiencies for exciplex fluorescence and cycloadduct formation are observed when exciplex specific quenchers are used.[41b,44,45] For anthracene/diene systems Yang has proposed that formation of Woodward–Hoffmann[46] (W–H) allowed, [4 + 4] or [2 + 2], and forbidden [4 + 2] products reflects competing concerted and stepwise collapse of singlet exciplexes,[42,43] whereas Kaupp favors direct formation of diradicals that either revert to ground-state addends or collapse to products.[46] Indirect evidence for the intermediacy of a reversibly formed exciplex in these cycloadditions has been reported for A/2,5-dimethyl-2,4-hexadiene,[47] A/DMH, and for 9,10-dichloroanthracene/1,3-

(33) Saltiel, J.; Townsend, D. E.; Sykes, A. *J. Am. Chem. Soc.* **1973**, *95*, 5968.
(34) Gorman, A. A.; Gould, I. R.; Hamblett, I. *J. Am. Chem. Soc.* **1981**, *103*, 4553.
(35) Saltiel, J.; Marchand, G. R.; Smothers, W. K.; Stout, S. A.; Charlton, J. L. *J. Am. Chem. Soc.* **1981**, *103*, 7159.
(36) Saltiel, J.; Shannon, P. T.; Zafiriou, O. C.; Uriarte, A. K. *J. Am. Chem. Soc.* **1980**, *102*, 6799.
(37) (a) Dawson, W. R.; Windsor, M. W. *J. Phys. Chem.* **1968**, *72*, 3251. (b) Birks, J. B.; Dyson, D. J. *Proc. R. Soc. London, Ser. A* **1963**, *275*, 135. (c) Weber, G.; Teale, F. W. J. *Trans. Faraday Soc.* **1957**, *53*, 646. (d) Melhuish, W. H. *J. Phys. Chem.* **1961**, *65*, 229.
(38) Horrocks, A. R.; Wilkinson, F. *Proc. R. Soc. London, Ser. A* **1968**, *306*, 257.
(39) Cohen, M. D.; Ludmer, A.; Yakhot, V. *Chem. Phys. Lett.* **1976**, *38*, 398.
(40) (a) Stephenson, L. M.; Whitten, D. G.; Vesley, G. F.; Hammond, G. S. *J. Am. Chem. Soc.* **1966**, *88*, 3665, 3893. (b) Stephenson, L. M.; Hammond, G. S. *Pure Appl. Chem.* **1968**, *16*, 125. (c) Stephenson, L. M.; Hammond, G. S. *Angew. Chem., Int. Ed. Engl.* **1969**, *8*, 261. (d) Evans, T. R. *J. Am. Chem. Soc.* **1971**, *93*, 2081. (e) Labianca, D. A.; Taylor, G. N.; Hammond, G. S. *Ibid.* **1972**, *94*, 3679. (f) Taylor, G. N.; Hammond, G. S. *Ibid.* **1972**, *94*, 3684, 3687.
(41) Taylor, G. N. *Chem. Phys. Lett.* **1971**, *10*, 355.
(42) Yang, N. C.; Yates, R. L.; Masnovi, J.; Shold, D. M.; Chiang, W. *Pure Appl. Chem.* **1979**, *51*, 173.
(43) Yang, N. C.; Srinivasachar, K.; Kim, B.; Libman, J. *J. Am. Chem. Soc.* **1975**, *97*, 5006.
(44) (a) Caldwell, R. A.; Smith, L. *J. Am. Chem. Soc.* **1974**, *96*, 2994. (b) Caldwell, R. A.; Creed, D.; DeMarco, D. C.; Melton, L. A.; Ohta, H.; Wine, P. H. *Ibid.* **1980**, *102*, 2369.
(45) (a) Majima, T.; Pac, C.; Sakurai, H. *Bull. Chem. Soc. Jpn.* **1978**, *51*, 1811. (b) Pac, C.; Sakurai, H. *Chem. Lett.* **1976**, 1067. (c) Itoh, M.; Takita, N.; Matsumoto, M. *J. Am. Chem. Soc.* **1979**, *101*, 7363.
(46) (a) Kaupp, G. *Angew. Chem., Int. Ed. Engl.* **1972**, *11*, 718. Also see: Kaupp, G. *Ibid.* **1972**, *11*, 313. (b) Kaupp, G.; Dyllick-Brenzinger, R.; Zimmerman, I. *Angew. Chem., Int. Ed. Engl.*, **1975**, *14*, 491. (c) Kaupp, G. *Liebigs Ann. Chem.* **1977**, 254. (d) Kaupp, G.; Gruter, H.-W. *Angew. Chem., Int. Ed. Engl.*, **1979**, *18*, 881.

cyclohexadiene, DCA/CH.[48] In both systems Stern–Volmer fluorescence quenching constants show inverse temperature dependencies.[47-49] This observation has furthermore been shown to account for the temperature dependence of $\phi_{t\text{-}4,4}$ for A/DMH.[47] In the DCA/CH case, pyridine, an exciplex-specific quencher,[44,45] markedly decreases adduct quantum yields.[48]

The fluorescence assigned to the exciplex in the A/D system[28] is far too weak to allow direct observation of the effect of quenchers on its behavior. However, since the presence of oxygen does not change the slopes of Stern–Volmer plots for anthracene fluorescence (I_0/I and τ_m^0/τ_m vs. [^{1}D]), either ^{1}(AD)* forms irreversibly or it is much shorter lived than the 27-ns decay time assigned to it.[28] The results in the present paper are in accord with a very short lifetime for the exciplex (see below).

In section B it was shown that A_2d arises solely from the quantitative thermal reaction of *t*-[4,4]Ad with A. The $\phi_{t\text{-}4,4}$ values in Table VII were therefore based on total A_2d yield measured by isotopic dilution following completion of the thermal reaction. According to Scheme I, the dependence of $\phi_{t\text{-}4,4}$ on [^{1}D] and [$\overline{^1A}$] is given by

$$\phi_{t\text{-}4,4}^{-1} = \alpha^{-1}\left(1 + \frac{1 + k_e\tau_m^0[\overline{^1A}]}{k_{ex}\tau_m^0[^1D]}\right) \quad (8)$$

where [$\overline{^1A}$] is the average concentration of ^{1}A, and α, the fraction of exciplexes which decay to *t*-[4,4]Ad, is the only unknown parameter. Using eq 8, we calculated α values for each $\phi_{t\text{-}4,4}$ entry in Table VII using the appropriate rate parameters in Table XIV. All values were in the range of 0.38–0.57 with seven of eleven defining the much narrower range 0.43–0.48; the average value, $\alpha = 0.46 \pm 0.02$ based on the latter, is entered in Table XIV. Lines for the highest and lowest [A]'s based on eq 8 are shown in Figure 2 together with selected experimental points. Interestingly, the value of α obtained is very close to that reported for the corresponding process in the A/DMH system in methylcyclohexane ($\alpha = 0.44 \pm 0.04$).[47] Aside from the fact that *t*-[4,4]Ad does not form in the fluorenone-sensitized reaction of A with D, its formation by a singlet pathway is clearly demonstrated by the observation that the presence of azulene, an efficient ^{3}A* quencher, does not alter $\phi_{t\text{-}4,4}$ (Table VII).

Though formation of [2,4]Ad occurs by reaction of either ^{1}A* or ^{3}A* with D, the very large difference in the lifetimes of these two excited states and the low reactivity of ^{3}A* make the triplet path much more sensitive to quenching interactions. Thus, $\phi_{2,4}$ values measured in the presence of air, azulene, or even at high [A] can be assigned exclusively to the singlet path, as can be seen by the absence of the triplet product x-Ad from GLC chromatograms under these conditions (Tables VIII and IX). According to Scheme I the dependence of $\phi_{2,4}$ on [^{1}D] in the presence of air or at high [^{1}A] is given by

$$\phi_{2,4}^{-1} = \beta^{-1}\left(1 + \frac{1 + k_e\tau_m[\overline{^1A}]}{k_{ex}\tau_m[^1D]}\right) \quad (9)$$

which is identical with eq 8 except that β is substituted for α and that in the presence of air $\tau_m = (k_f + k_{is} + k_{qs}[O_2])^{-1} = \tau_m^0/1.19$ replaces τ_m^0. The $\phi_{2,4}$ values for air-saturated solutions and for degassed solutions and $[A]_0 \simeq 8.3 \times 10^{-3}$ M are plotted according to eq 9 in Figure 3 and give $\beta = 0.08_9 \pm 0.01$ and $\beta = 0.07_6 \pm 0.01$, respectively. The fact that, if anything, a larger value of β is obtained in the presence of air justifies the omission from the mechanism of ^{1}(AD)* quenching by O_2. Such quenching would be pronounced indeed if the lifetime of the exciplex were 27 ns, and it is therefore concluded that our report of this lifetime is in error. The two sets of experiments taken together suggest that $\beta = 0.08 \pm 0.02$ (Table XIV). The ratio α/β from the quantum yield experiments is in very good agreement with the ratio observed

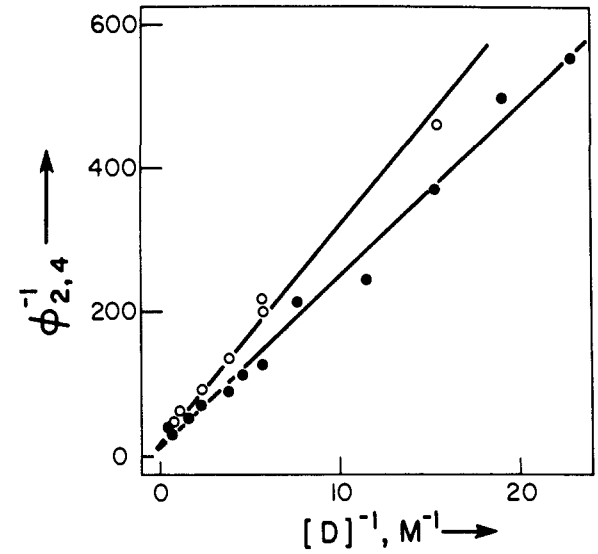

Figure 3. Diene concentration dependence of $\phi_{2,4}$ at high (○) [^{1}A] and at low (●) [^{1}A] in the presence of air (eq 9).

Scheme II

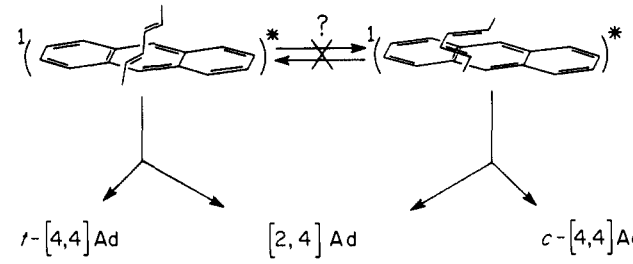

in ^{1}H NMR spectra of product mixtures from preparative experiments. Since no quantum yields are available for *c*-[4,4]Ad, $\gamma = 0.02_5 \pm 0.010$ is based entirely on the ^{1}H NMR spectra. The ratio α/γ is close to that expected for the *s-trans*-D/*s-cis*-D ratio[50] and may reflect formation of isomeric exciplexes from the two D conformers (Scheme II).

The presence of air eliminates both the triplet pathway to cross-adducts and the TTA pathway to A_2. Under these conditions ϕ_{A_2} values are given by

$$(\phi_{A_2})_{air} = \frac{p_{ed}k_e\tau_m[\overline{^1A}]}{1 + k_e\tau_m[\overline{^1A}] + k_{ex}\tau_m[O_2]} \quad (10)$$

where τ_m is (τ_m^0/1.19) as in eq 9. Total quantum yields of cross-adducts under these conditions, $(\phi_{Ad})_{air}$, obtained by subtracting $2(\phi_{A_2})_{air}$ from the ϕ_{-A} values in Table VI, are listed in Table VI.

$$(\phi_{Ad})_{air} = (\phi_{-A})_{air} - 2(\phi_{A_2})_{air} \quad (11)$$

The dependence of $(\phi_{Ad})_{air}$ on [$\overline{^1A}$] and [^{1}D] can be calculated from eq 9 by replacing β^{-1} with $(\alpha + \beta + \gamma)^{-1}$. Expected lines for the three sets of A concentrations are drawn in Figure 4 by using $(\alpha + \beta + \gamma) = 0.56_5$ derived above. The $(\phi_{Ad})_{air}$ values adhere very closely to the expected behavior and provide an independent confirmation of the analysis of individual adduct quantum yields. The assumption that the exciplex is too short-lived to be quenched by oxygen is also confirmed since the presence of air produces no detectable effect on α.

(c) The Triplet Pathway to Cross-Adducts. Ample evidence that acenaphthylene[51] and phenanthrene[52] triplets undergo cy-

(47) Yang, N. C.; Shold, D. M. *J. Chem. Soc., Chem. Commun.* **1978**, 978.
(48) Smothers, W. K.; Meyer, M. C.; Saltiel, J. *J. Am. Chem. Soc.* **1983**, *105*, 545.
(49) Stevens, B.; Ban, M. I. *Trans. Faraday Soc.* **1964**, *60*, 1515.
(50) Pui, P. W.; Grunwald, E. *J. Am. Chem. Soc.* **1982**, *104*, 6562 and references cited.
(51) Ferree, W. I., Jr.; Plummer, B. F.; Schloman, W. W., Jr. *J. Am. Chem. Soc.* **1974**, *96*, 7741, and other papers in this series.
(52) (a) Caldwell, R. A. *J. Am. Chem. Soc.* **1973**, *95*, 1690. (b) Caldwell, R. A.; Creed, D. *Ibid.* **1977**, *99*, 8360. (c) Caldwell, R. A.; Creed, D.; Maw, T.-S. *Ibid.* **1979**, *101*, 1293.

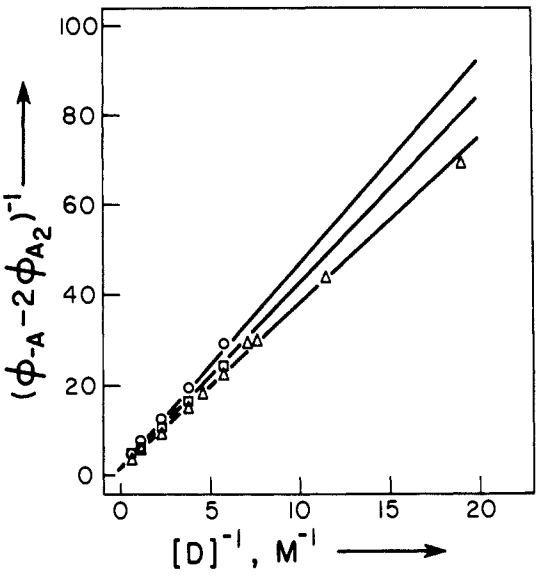

Figure 4. Diene concentration dependence of $(\phi_{Ad})_{air}$ at high (○), medium (□), and low (△) [^{1}A] (eq 10 and 11).

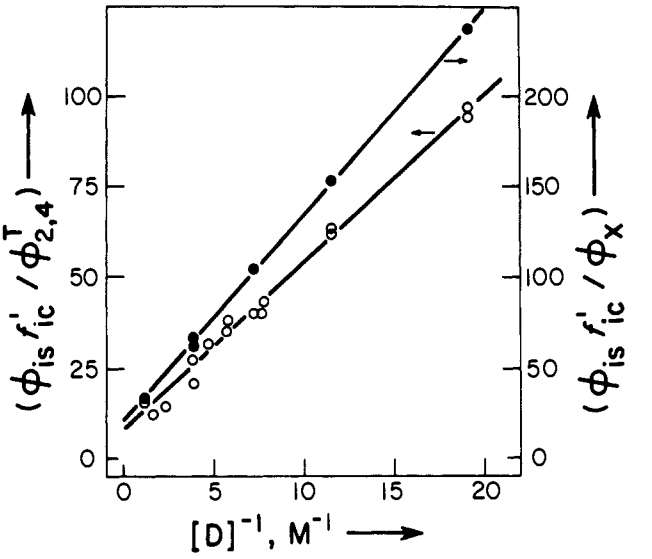

Figure 5. Diene concentration dependence of $\phi_{2,4}{}^T$ (○) and ϕ_x (●) for direct excitation of A (eq 12–14).

cloaddition to olefins has been presented. For the present work, the nonstereospecific addition of 1,2-benzanthracene triplets to the 1,3-pentadienes, which gives [2 + 4] adducts across the 9,10 positions of the anthracene moiety, provides an especially relevant precedent.[53] The mechanism of these reactions is generally considered to involve relatively long-lived triplet biradical intermediates, which intersystem cross before, or as, they collapse to products. The stepwise addition allows for the formation of products that would be otherwise W–H forbidden. As expected, product structures show that when acyclic 1,3-dienes are employed as the olefin partner, allyl units in the biradicals retain their stereochemistry.[51,53]

The fluorenone-sensitized experiments establish [2,4]-Ad and x-Ad (more than one adduct with the same GLC retention time could account for the peaks assigned to [2,4]-Ad and x-Ad) as the major cross-adducts of the triplet pathway, Table X. When A is excited directly, the presence of triplet quenchers, O_2 or Az, eliminates x-Ad and markedly attenuates the yield of [2,4-Ad] in the product mixture (Tables VIII and IX). On the other hand, the presence of MeI reduces $\phi_{t\text{-}4,4}$ more than tenfold, while nearly doubling $\phi_{2,4}$ and ϕ_x (Tables VIII and IX).

According to Scheme I, the dependence of triplet cross-adduct quantum yields, $\phi_{Ad}{}^T$, on reactant concentrations for direct excitation conditions is, to a good approximation, given by

$$(\phi_{Ad})^T = \phi_{is} f_{ic}(\delta + \epsilon)\frac{k_{qd}[D]}{k_{dt}{}^0 + k_{sq}[^1A] + k_{qd}[^1D]} \qquad (12)$$

where ϕ_{is}, the intersystem crossing quantum yield, decreases as [^{1}D] and [^{1}A] are increased

$$\phi_{is} = \frac{k_{is}\tau_m{}^0}{1 + k_e\tau_m{}^0[^1A] + k_{ex}\tau_m{}^0[^1D]} \qquad (13)$$

and f_{ic} gives the efficiency of the $^3A^{**} \rightarrow {}^3A^*$ process as a function of [^{1}D]. The relationship is approximate because it disregards the second-order TTA component in the decay of ^{3}A*. This component, of course, is diminished by D due to the latter's contribution in decreasing ϕ_{is} and increasing k_{dt}. It could be included by basing $(\phi_{Ad})^T$ on $[^3A^*]_{ss}$, eq 6, as was done for ϕ_{A_2}, but the accuracy of the adduct quantum yields is not sufficient to justify this added complexity. One of the difficulties in fitting the data to eq 12 has been mentioned. It concerns the degree to which the back-energy-transfer step, eq 7, modifies f_{ic}. By analogy with 2,5-dimethyl-2,4-hexadiene triplets,[34] it seems likely that the rate constant for excitation transfer from ^{3}D* to ^{1}A should be about half the rate constant for diffusion. It follows that approximately half of the cage pairs in eq 7 should undergo excitation transfer before diffusing apart and that f_{ic} in eq 6 and 12 should be replaced with $f_{ic}' = f_{ic} + 0.5(1 - f_{ic})$. The second difficulty concerns the effect of residual oxygen on the magnitude of k_{dt}. In numerous flash kinetic experiments we have found that even when extreme care in degassing is taken (more than 12 freeze–pump–thaw cycles before sealing) k_{dt} values of 100–200 s^{-1} are achieved, always higher than the limiting $k_{dt}{}^0 \simeq 50$ s^{-1}.[29] Since only 5–6 freeze–pump–thaw cycles were employed for photochemical experiments, a somewhat larger effective "$k_{dt}{}^0$" value is expected and this quantity is best treated as an adjustable parameter.

Since x-Ad forms only by the triplet pathway, application of the rearranged form of eq 12

$$\frac{\phi_{is} f_{ic}'}{\phi_{x\text{-}Ad}} = \frac{1}{\epsilon}\left(1 + \frac{k_{dt}{}^0 + k_{sq}[^1\overline{A}]}{k_{qd}[^1D]}\right) \qquad (14)$$

is straightforward. Values of ϕ_{is} and f_{ic}' were calculated for each [^{1}D], using rate parameters from Table XIV, and the quantity on the left of the equal sign in eq 14 was plotted vs. $[^1D]^{-1}$ (Figure 5, only ϕ_x values from GLC procedure 2 were treated). The adherence to the straight line is remarkably good ($r^2 = 0.999$) and gives $\epsilon = 0.047$ and "$k_{dt}{}^0$" = 325 s^{-1}, a reasonable value.

Singlet contributions, $\phi_{2,4}{}^S$, of $\phi_{2,4}$ under degassed conditions were calculated by using $\beta = 0.08_9$ obtained from experiments carried out in parallel with air-saturated solutions and substituting $\tau_m{}^0$ for τ_m in eq 9. Subtraction of $\phi_{2,4}{}^S$ values from the experimental values (Table VIII) yields triplet contributions, $\phi_{2,4}{}^T$, which are plotted in Figure 5 employing eq 14 with δ substituted for ϵ. Least-squares treatment of the data (excluding highest $\phi_{2,4}$ value at 0.263 M D) gives $\delta = 0.122$ and "$k_{dt}{}^0$" = 280 s^{-1}. The results of this treatment are rather sensitive to the value of β employed in eq 9. For instance, for $\beta = 0.080$ the same procedure gives $\delta = 0.133$ and "$k_{dt}{}^0$" = 385 s^{-1}. The δ/ϵ ratio obtained 2.6–2.8 is therefore considered to be in satisfactory agreement with that observed with fluorenone as the triplet energy donor, 3.2 ± 0.2 (Table X, see below also). An effective "$k_{dt}{}^0$" in the 300–500-s^{-1} range suggests that $\sim 10^{-7}$ M was the residual [O_2] achieved by our degassing. The extent to which the triplet pathway contributes to adduct formation is very sensitive to the overall size of k_{dt}. This explains why the triplet pathway did not contribute significantly in preparative experiments in which high $[^1A]_0$ were usually employed and removal of O_2 was by bubbling of N_2 or Ar through the solutions. Similarly, the effect of Az is the complete elimination of the triplet pathway even at the lowest concentration

(53) Saltiel, J.; Townsend, D. E.; Metts, L. L.; Wrighton, M.; Mueller, W.; Rosanske, R. C. *J. Chem. Soc., Chem. Commun.* **1978**, 588.

employed (Table IX). It can be seen that the drop in ϕ_{-A}^0 is accounted for completely, within experimental uncertainty, by the reduction in $\phi_{2,4}$ and the elimination of x-Ad as a product. Triplet excitation transfer from $^3A^*$ to Az is known to be diffusion-controlled.[54]

A general trend of *decreasing* [4,4]Ad/[2,4]Ad product ratios with *increasing* arene concentration has been based on preparative experiments with several arene/diene systems.[55] It was proposed that monomer arene excited singlets are more prone to concerted [4,4] adduct formation than are arene singlet excimers, which being less reactive tend to undergo stepwise [2 + 4] addition as a consequence of the interaction described in eq 2. The present system provides an important exception to this trend. An *increase* in $\phi_{t\text{-}4,4}/\phi_{2,4}$ with *increasing* $[^1A]_0$ is observed that is accounted for quantitatively by the suppression of the triplet path to [2,4]Ad due to self-quenching of $^3A^*$.

Quenching of fluorenone triplets, $^3Fl^*$, E_T = 53 kcal/mol,[56] is highly exothermic and should be diffusion-controlled, $k_{FA} = k_{diff}$.[54]

$$^3Fl^* + {}^1A \xrightarrow{k_{FA}} {}^1Fl + {}^3A^* \qquad (15)$$

However, D is expected to compete with A for $^3Fl^*$ in a process known to give primarily s-cis triplets.[23]

$$^3Fl^* + {}^1D \xrightarrow{k_{FD}} {}^1Fl + s\text{-}cis\text{-}{}^3D^* \qquad (16)$$

The competition is reflected in quenching of the fluorenone-sensitized tt → ct photoisomerization of D by A

$$(\phi_{tt\rightarrow ct}^0/\phi_{tt\rightarrow ct}) = 1 + (k_{FA}[^1A]/k_{FD}[^1D]) \qquad (17)$$

where $\phi_{tt\rightarrow ct}^0$ is the known limiting quantum yield[23] in the absence of A. By using eq 17 the data in Table XI give $(k_{FA}/k_{FD}) = 2.1 \times 10^2$, a reasonable value when one considers the low ground-state population of *s-cis*-D conformers[50] and the expectation that excitation transfer from $^3Fl^*$ to *s-cis*-^{1}D should be close to isoenergetic.[23] This ratio also determines the efficiency of $^3A^*$ formation in the initial sensitization step for cycloaddition, $f_{et} = k_{FA}[^1A]/(k_{FA}[^1A] + k_{FD}[^1D])$. However, since excitation transfer from *s-cis*-^{3}D* to ^{1}A should be exothermic, the full efficiency of $^3A^*$ formation must include

$$s\text{-}cis\text{-}{}^3D^* + {}^1A \rightarrow tt\text{-}D + ct\text{-}D + {}^3A^* \qquad (18)$$

the diffusional counterpart of eq 7 (neglected earlier in the estimation of f_{ic}' because of lower [A] values). Recognizing that the analogy with 2,5-dimethyl-2,4-hexadiene[34] is weaker because s-cis triplets are involved, a 50-ns lifetime for *s-cis*-^{3}D* and an excitation transfer rate constant of 4×10^9 M^{-1} s^{-1} for eq 18 were assumed to estimate $f_{et}' = f_{et} + 0.35(1 - f_{et})$ for the concentrations employed in the sensitized cycloaddition experiments. The dependence of adduct quantum yields on reactant concentrations under these conditions is given by

$$\frac{f_{et}'\phi_{is}^F}{\phi_{2,4 \text{ or } x}} = \frac{1}{(\delta \text{ or } \epsilon)}\left(1 + \frac{k_{dt}^0 + k_{sq}\overline{[^1A]}}{k_{qd}[^1D]}\right) \qquad (19)$$

where $\phi_{is}^F = 0.93$ is the intersystem crossing efficiency of fluorenone.[57] As before, fitting the data to eq 19 is difficult because the degree to which "k_{dt}^0" is enhanced by impurity quenching, including possible quenching of $^3A^*$ by Fl, is unknown. The quantum yields in Table X are plotted according to eq 19 in Figure 6. Least-squares lines were drawn through the four highest [D] points after imposing the added restriction that the intercepts be roughly consistent with δ and ϵ obtained from the direct excitation experiments (see above). A good fit is obtained with $\delta = 0.14$, $\epsilon = 0.045$, and "k_{dt}^0" = 220 s^{-1}. The points for [D] = 0.140 M fall considerably above the lines and if included in the treatment suggest "k_{dt}^0" = 430 s^{-1}. These results are therefore consistent with the interpretation of the triplet adduct quantum yields for the direct excitation experiments.

Equation 19 is approximate because it does not account for the TTA part of $^3A^*$ decay. This part is responsible for the "singlet products" A_2 and *t*-[4,4]Ad for which yields are also reported in Table X. The first three rows in the table in the absence of D illustrate the sharp reduction of ϕ_{A_2} as the self-quenching term in the decay rate of $^3A^*$ is increased. In the same way, the presence of D also reduces the contribution of the TTA pathway to products. In fact, it can be seen that for the four highest $[^1D]$ with $[^1A] \simeq 2.7 \times 10^{-3}$ M the cross-adduct quantum yields account for essentially all of the A loss. The small values of ϕ_{A_2} and $\phi_{t\text{-}4,4}$ obtained by isotopic dilution, though not considered reliable because the number of counts above background was small, are roughly consistent with those expected from TTA (note, however, the unexpected *increase* in $\phi_{t\text{-}4,4}$ with *decreasing* I_a). The small contribution of *t*-[4,4]Ad in the photoproducts of the sensitized reaction was evident in our inability to detect by UV measurements any A loss from thermal A_2d formation following the irradiations.

(d) The External Heavy-Atom Effect. That interaction of solute molecules with molecules containing heavy atoms increases the probabilities of radiative and nonradiative singlet–triplet transitions is well established by spectroscopic observations.[58] This phenomenon is known as the external heavy-atom effect and is attributed to induced spin–orbital coupling. In photochemistry, it enhances yields of triplet-derived products.[51,59] The influence of heavy-atom addends on acenaphthylene photodimerization[59] and cross-adduct formation[51] is especially well understood. The dependence of photodimerization quantum yields on ethyl iodide, EtI, concentration in cyclohexane provides an excellent precedent for our results.[59c] The quantum yields increase rapidly at low [EtI], reach a maximum value at about 10 mol %, and then decrease slowly as [EtI] is increased to 100 mol %. Heavy-atom induced $S_1 \rightarrow T_1$ intersystem crossing is responsible for the initial increase, while the decrease at higher concentrations is due to significant, though much less pronounced, induced $T_1 \rightarrow S_0$ intersystem crossing.[59c] Qualitative observations suggest that similar effects influence the photochemistry of A/1,3-cyclohexadiene and A/1,3,5-cycloheptatriene.[42] Addition of MeI in either benzene or acetonitrile as cosolvent increases the relative yields of [2 + 4] cross-adducts in these systems.[42] However, since the overall quantum efficiency of product formation is appreciably reduced by MeI, it is not clear whether the change in product distributions represents selective quenching of singlet pathways, enhancement of triplet pathways, or both. Our own experience suggests that rigorous degassing is essential for triplets to contribute to product formation. More definitive are spectroscopic results that indicate EtI induces both $S_1 \rightarrow T$ and $T_1 \rightarrow S_0$ intersystem crossing in A[60]

$$^1A^* + RI \xrightarrow{k_{ha}^S} {}^3A^* + RI \qquad (20)$$

$$^3A^* + RI \xrightarrow{k_{ha}^T} {}^1A + RI \qquad (21)$$

Also, the presence of a reversibly formed A/EtI triplet exciplex was inferred from triplet lifetime measurements that suggest cooperative quenching of $^3A^*$ by EtI and ferrocene.[60b]

Under our conditions the value of k_{ha}^S can be estimated from the effect of MeI on $^1A^*$ fluorescence (Table XII). A slight upward curvature in the Stern–Volmer plot was considered to be negligible due to the uncertainty in the I_0/I values; however, it

(54) Herkstroeter, W. G. *J. Am. Chem. Soc.* **1975**, *97*, 4161.
(55) Yang, N. C.; Shou, H.; Wang, T.; Masnovi, J. *J. Am. Chem. Soc.* **1980**, *102*, 6652.
(56) Herkstroeter, W. G.; Hammond, G. S. *J. Am. Chem. Soc.* **1966**, *88*, 4769. Cf., however: Yoshihara, K.; Kearns, D. R. *J. Chem. Phys.* **1966**, *45*, 1991 where E_t = 50 kcal/mol is given.
(57) Lamola, A. A.; Hammond, G. S. *J. Chem. Phys.* **1965**, *43*, 2129.
(58) (a) Lower, S. K.; El-Sayed, M. A. *Chem. Rev.* **1966**, *66*, 199. (b) McGlynn, S. P.; Azumi, T.; Kinoshita, M. *Molecular Spectroscopy of the Triplet State*; Prentice-Hall: Englewood Cliffs, NJ, 1969. (c) Birks, J. B. *Photophysics of Aromatic Molecules*; Wiley-Interscience: New York, 1970. (d) Wilkinson, F. *Organic Molecular Photophysics*; Birks, J. B., Ed.; Wiley-Interscience: New York, 1975; Vol. 2, p 95.
(59) (a) Cowan, D. O.; Drisko, R. L. *Tetrahedron Lett.* **1967**, 1255. (b) Cowan, D. O.; Drisko, R. L. *J. Am. Chem. Soc.* **1967**, *89*, 3068; **1970**, *92*, 6281, 6286. (c) Cowan, D. O.; Koziar, J. C. *J. Am. Chem. Soc.* **1974**, *96*, 1229; **1975**, *97*, 249. (d) Cowan, D. O.; Drisko, R. L. *Elements of Organic Photochemistry*; Plenum Press: New York, 1976.
(60) (a) DeToma, R. P.; Cowan, D. O. *J. Am. Chem. Soc.* **1975**, *97*, 3283. (b) Tamargo, M. C.; Cowan, D. O. *Ibid.* **1982**, *104*, 1107; **1985**, *107*, 1457.

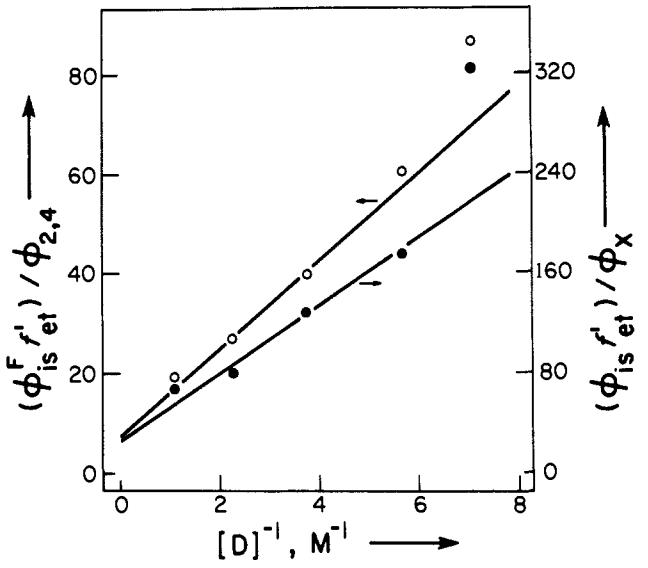

Figure 6. Diene concentration of $\phi_{2,4}$ (○) and ϕ_x (●) for the fluorenone-sensitized reaction (eq 19).

could be due to a small static contribution to the quenching (cf. ref 4 for a related case, where static quenching is definitely established). The least-squares line of the Stern–Volmer plot, forced through unity as the intercept, gives $k_{ha}{}^S\tau_m = 19.3$ ($r^2 = 0.993$). With use of the lifetime of $^1A^*$ in the presence of air, $k_{ha}{}^S = 5.5 \times 10^9$ M^{-1} s^{-1} at 23 °C in benzene is obtained which is in reasonable agreement with $k_{ha}{}^S = 3.96 \times 10^9$ M^{-1} s^{-1} measured for EtI in cyclohexane.[60a] (If the initial slope of our Stern–Volmer plot were employed, the $k_{ha}{}^S$ value drops to 3.9×10^9 M^{-1} s^{-1}.) Since our value indicates eq 20 to be nearly fully diffusion-controlled ($k_{ha}{}^S \simeq 0.64\ k_{diff}$), $k_{ha}{}^S$ was adjusted to 30 °C for the change in T/η leading to 6.1×10^9 M^{-1} s^{-1}.

Equation 8 with $\alpha = 0.46$ predicts $\phi_{t\text{-}4,4} = 0.150$ in the absence of MeI for [^{1}A] and [^{1}D] values employed in our experiment (compare with $\phi_{-A}{}^\infty - \phi_{-A}{}^0 = 0.132$ in Table IX). Since *t*-[4,4]Ad is derived solely from $^1A^*$, a sharp drop in $\phi_{t\text{-}4,4}$ was expected in the presence of MeI. This is confirmed by the isotopic dilution based $\phi_{t\text{-}4,4}$ values at 0.642 and 1.28 M MeI which are lower by factors of 27 and 54, respectively, than $\phi_{t\text{-}4,4}$ in the absence of MeI (Table IX). Assuming that eq 20 describes the only process by which MeI interferes with *t*-[4,4]Ad formation, the dependence of $\phi_{t\text{-}4,4}$ on [MeI] is given by

$$\phi_{t\text{-}4,4} = \frac{\alpha k_{ex}\tau_m{}^0[^1D]}{1 + k_e\tau_m{}^0[\overline{^1A}] + k_{ex}\tau_m{}^0[^1D] + k_{ha}{}^S\tau_m{}^0[MeI]} \quad (22)$$

Actually, the experimental $\phi_{t\text{-}4,4}$ values are more than a factor of 2 smaller than predicted by eq 22, possibly indicating that the high [MeI] employed are sufficient to quench ^{1}(AD)*

$$^1(AD)^* + MeI \xrightarrow{k_{ha}{}^{Ex}} {}^3(AD)^* + MeI \quad (23)$$

This process would lead to a decrease in α with increasing [MeI] and would accommodate the low observed $\phi_{t\text{-}4,4}$. If, furthermore, it were assumed that $k_{ha}{}^S = k_{ha}{}^{Ex}$, a short exciplex lifetime, $\tau_{ex} = 0.2$ ns, would be predicted, consistent with the absence of O_2 and Az quenching of ^{1}(AD)*. The MeI data may therefore provide evidence that the exciplex is an essential intermediate in *t*-[4,4]Ad formation. However, the conclusion is tentative because a factor of 2 error in $\phi_{t\text{-}4,4}$ is not out of the question. Due to the small yields involved, scintillation counting measurements for A_2d gave counting rates only slightly above background (86 and 37% at 0.64_2 and 1.28 M MeI, respectively).

Sensibly, the decrease in $\phi_{t\text{-}4,4}$ with [MeI] is accompanied by a large increase in the quantum yields of the triplet-derived adducts (Table IX). The changes in $\phi_{2,4}$ and ϕ_x with [MeI] are analogous to those observed in acenaphthylene dimer quantum yields.[59c] Maximum values are attained at the lowest [MeI] employed (0.161 M), followed by a plateau region and a slow decrease as [MeI] is increased. As in the acenaphthylene case the sharp initial increase can be attributed to enhanced $^3A^*$ yields through step 20, while the eventual decrease (moderated perhaps by step 23 at higher [MeI]) reflects the shortening of the effective $^3A^*$ lifetime through step 21. The change in the $\phi_{2,4}/\phi_x$ ratio may be analogous to the change in syn/anti acenaphthylene dimer ratio that was attributed to changes in medium polarity.[59c] Changes in adduct distributions in A/D systems with solvent change have also been noted (cf., however, ref 48).[42,43] Quantitative interpretation of triplet adduct quantum yields ($\phi_{2,4}{}^T + \phi_x = \phi_{Ad}{}^T$) can be based on

$$\phi_{Ad}{}^T = \frac{\phi_{is}{}^{ha} f_{ic}'(\delta + \epsilon)k_{qd}[^1D]}{k_{dt}{}^0 + k_{sq}[^1A] + k_{qd}[^1D] + k_{ha}{}^T[MeI]} \quad (24)$$

where

$$\phi_{is}{}^{ha} = \frac{k_{is}\tau_m{}^0 + k_{ha}{}^S\tau_m{}^0[MeI]}{1 + k_e\tau_m{}^0[^1A] + k_{ex}\tau_m{}^0[^1D] + k_{ha}{}^S\tau_m{}^0[MeI]} \quad (25)$$

These expressions are modified versions of eq 12 and 13. They neglect the possible small contribution of eq 23 to adduct formation, as well as the influence (minor at high [^{1}D]) of TTA on the lifetime of $^3A^*$. No heavy-atom effect on f_{ic}' is expected in view of the short lifetime of $^3A^{**}$ and the large electronic energy gap separating it from the ground state. Rearrangement of eq 24 gives

$$\frac{\phi_{is}{}^{ha} f_{ic}'}{\phi_{Ad}{}^T} = \left(\frac{1}{\delta + \epsilon}\right)\left(\frac{k_{dt}{}^0 + k_{sq}[^1A] + k_{qd}[^1D]}{k_{qd}[^1D]} + \frac{k_{ha}{}^T[MeI]}{k_{qd}[^1D]}\right) \quad (26)$$

Singlet contributions to [2,4]Ad, estimated by using eq 22, with $\beta = 0.08_9$ substituted for α, were subtracted from ($\phi_{2,4} + \phi_x$) in Table IX. A plot of the resulting $\phi_{Ad}{}^T$ according to eq 26 is linear with $i = 6.08$ and $s = 2.94$ ($r^2 = 0.994$). Interpretation of these values is again hampered by uncertainty in "$k_{dt}{}^0$". However, assuming "$k_{dt}{}^0$" in the 50–400-s^{-1} range gives ($\delta + \epsilon$) = 0.21–0.28 from i and $k_{ha}{}^T = (5.5\text{–}7.1) \times 10^2$ $M^{-1}s^{-1}$ from s/i. The range for ($\delta + \epsilon$) is in good agreement with ($\delta + \epsilon$) $\simeq 0.18$ obtained from the treatment of direct and sensitized experiments in the absence of MeI (see above). However, the estimated range for $k_{ha}{}^T$ indicates that it is much smaller than values reported for EtI in cyclohexane ($k_{ha}{}^T = 6.95 \times 10^4$ M^{-1} s^{-1})[60a] and in methylcyclohexane ($k_{ha}{}^T = 5.35 \times 10^3$ M^{-1} s^{-1}).[60b] Our own flash-kinetics determinations of rate constants for MeI and EtI are in progress, and initial observations suggest that $k_{ha}{}^T$ is in the 600–1000 M^{-1} s^{-1} range,[61] in agreement with the photochemical data. An independent test of the validity of the adduct yields used in Figure 7 is furnished by the ϕ_{-A} values which agree with values predicted by the product quantum yields.

Under the conditions of this experiment, but in the absence of MeI, $\phi_{A_2} = 2.96 \times 10^{-3}$ (97% from the direct singlet route and 3% from TTA) is predicted by eq 5 and 6, see part Ca. $^1A^*$, and hence the direct path to A_2, should be strongly quenched by MeI (by more than a factor of 10). It is remarkable, therefore, that ϕ_{A_2} at 0.64 and 1.28 M MeI remains essentially unaffected (Table IX). Again, the small activities encountered in the scintillation counting measurements (38 and 31% over background) suggest caution in the interpretation of these results. However, explanations such as (a) interception of the, thus far elusive, triplet excimer by MeI and (b) increase in p_e' in eq 5 due to MeI-induced spin–orbital coupling between spin-states of triplet–triplet encounter pairs are intriguing possibilities and are the subject of current research in our laboratory.[61]

(e) Total A Loss. As an additional test of the derived parameters α, β, γ, δ, and ϵ and the mechanism in Scheme I, total anthracene loss quantum yields were calculated as a function of [D] by summing contributions to A loss due to dimerization ($2\phi_{A_2}$

(61) Saltiel, J.; Ganapathy, S., unpublished results.

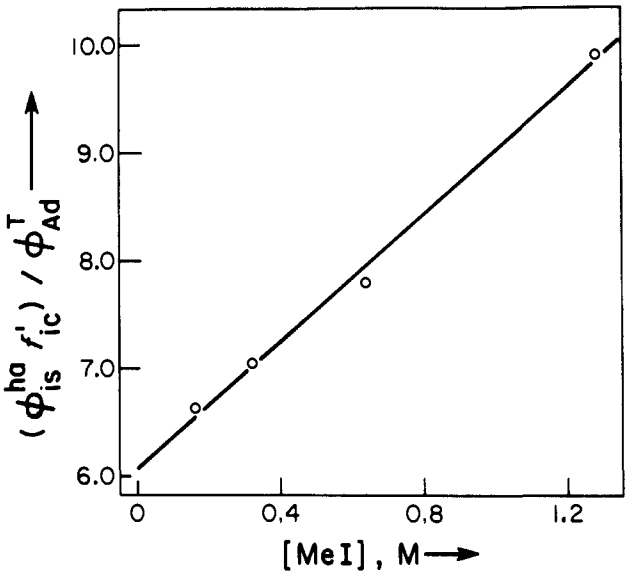

Figure 7. MeI concentration dependence of $\phi_{Ad}{}^{T}$ (eq 26).

from eq 5 and 6), the singlet pathway to adducts ($\phi_{Ad}{}^{S}$ from eq 8 with $(\alpha + \beta + \gamma) = 0.56_5$), and the triplet pathway to adducts ($\phi_{Ad}{}^{T}$ from eq 14 with $(\delta + \epsilon) = 0.18$ and "$k_{dt}{}^{0}$" = 350 s^{-1}). The separate contributions and the calculated total ϕ_{-A} values are plotted in Figures 8 and 9 for the sets of lowest and highest [A] employed, respectively. The points are experimental ϕ_{-A} values from Table V. The agreement is gratifying, especially since the quantum yields in Table V were not used in the derivation of any of the parameters.

As expected, the contribution of the triplet pathway to adducts, although small, is much more significant at low [A]. A somewhat larger contribution by $\phi_{Ad}{}^{T}$ than shown in Figures 8 and 9 is predicted for more rigorously degassed solutions in which "$k_{dt}{}^{0}$" should approach its true unimolecular value of ~50 s^{-1}. The $\phi_{2,4}$ values for ~8.3 × 10^{-3} M $[A]_0$ (Table VIII) demonstrate that our degassing procedure did not uniformly achieve an $[O_2]$ level consistent with "$k_{dt}{}^{0}$" ≃ 350 s^{-1}. The calculated ϕ_{Ad}'s shown in Figure 9 indicate that the triplet pathway to [2,4]Ad for "$k_{dt}{}^{0}$" ≃ 350 s^{-1} should have been significant. However, the absence of x-Ad and the magnitude of the measured $\phi_{2,4}$ suggest that only the singlet pathway gave adducts, consistent with our treatment of the data in Figure 3. It is likely that an unusually large value of "$k_{dt}{}^{0}$" in this experiment accounts for these results.

(D) Summary. Scheme I quantitatively accounts for the photochemistry of the A/D system in benzene over the entire concentration range employed. Product-forming steps involving encounters between ^{1}(AA)* or ^{1}(AD)* with either ^{1}A or ^{1}D are strictly ruled out in this system. High A losses, previously attributed to eq 3, are due to thermal reaction between *t*-[4,4]Ad and A, subsequent to the irradiation, as proposed by Kaupp.[14] The structure of the thermal product A_2d was established by X-ray crystallography.

The singlet pathway to adducts gives mainly [$4_\pi + 4_\pi$] products, presumably by concerted W–H allowed collapse of isomeric ^{1}(AD)* exciplexes (Scheme II). It is likely that the exciplexes are reversibly formed and, if so, are too short-lived to be quenched by O_2 or Az ($\tau_{ex} < 1$ ns). A significant fraction (14%) of product-forming steps from ^{1}(AD)* leads to [2,4]Ad. Whether this reaction is a concerted W–H forbidden process or is stepwise is unknown at this time. However, if a singlet biradical intermediate is involved, its collapse to [2,4]Ad must be extremely fast since ^{1}H NMR spectra of singlet adduct mixtures indicate the formation of a single [$2_\pi + 4_\pi$] stereoisomer.

[2,4]Ad is the major product from the triplet pathway to adducts. Since this pathway very likely involves a triplet biradical intermediate, it sensibly gives no [$4_\pi + 4_\pi$] adducts. The identity of minor adducts from this pathway was not determined; however, ^{1}H NMR spectra of product mixtures are consistent with the presence of stereoisomers of [2,4]Ad.

The role of the external heavy-atom effect in adduct formation was unequivocally established. MeI quenches singlet adduct formation and enhances formation of triplet adducts.

Experimental Section

Materials. Most materials and purification procedures have been described in ref 5, 27, and 28. Alternative sources and additional material used in this work were as follows. Anthracene (Eastman, Practical grade) was chromatographed on alumina, recrystallized from *n*-hexane twice, and sublimed under reduced pressure, mp 216.5–217.5 °C. Anthracene-^{14}C was synthesized[62] from benzene-^{14}C (New England Nuclear) and phthalic anhydride (Mallinckrodt, Analytical reagent) which had been recrystallized twice from chloroform and dried under vacuum, mp 132.0–132.5 °C. Fluorenone (Matheson, Coleman and Bell) was recrystallized twice from toluene and sublimed under reduced pressure, mp 83.5–84.0 °C. Xanthone (Aldrich, Research grade) was recrystallized from *n*-hexane three times and vacuum sublimed, mp 174.5–175.0 °C. *p*-Bis[2-(5-phenyloxazolyl)]benzene, POPOP (Pilot Chemicals), mp 244.0–245.0 °C, and 2,5-diphenyloxazole, POP (Eastman, Analytical reagent), were used as received. Azulene (Aldrich, 99.6%) was used as received. Methyl iodide (Fisher, Certified reagent) was distilled over mossy zinc, bp 41 °C, and then bulb-to-bulb distilled under reduced pressure. Benzene (Mallinckrodt, Reagent grade) was purified by the Metts exhaustive photochlorination procedure.[35,63]

Fluorescence Measurements. A Hitachi Perkin-Elmer MPF-2A spectrophotometer equipped with an Osram 150-W Xenon lamp and R-106 photomultiplier was employed in the ratio recording mode. Data were collected by slow scanning (100 ms/point) on a Nicolet-Explorer I digital storage oscilloscope. Hard copy output was obtained as digital intensity vs. wavelength with use of a Hewlett-Packard Model 2D-2M X-Y recorder. Spectra were recorded for air-saturated solutions at ambient temperature (~23 °C) with use of 1 × 1 cm quartz cells fitted with tapered Teflon stoppers.

Absorption Measurements. UV spectra were recorded at room temperature on Cary 14, 15, and 219 spectrophotometers. At the last stages of this work a Perkin-Elmer Lambda-5 spectrophotometer was employed. Pyrex sidearm cells were custom made and were calibrated with known solutions of A before use; otherwise standard quartz cells were employed. NMR spectra were obtained on Bruker HX-270 or Bruker-IBM WP-Y-200 MHz instruments with tetramethylsilane as internal standard. IR spectra were obtained on a Perkin-Elmer Model 137 sodium chloride prism spectrophotometer.

Gas–Liquid Chromatography. GLC conditions for isomeric compositions of the hexadienes[64] and the stilbenes[20] have been described previously. A Varian-Aerogaph Model 940 instrument with hydrogen flame detector was employed for hexadiene composition analyses.[64] Adduct compositions were determined on a Varian-Aerograph Model 2700 instrument equipped with dual/differential electrometer and flame ionization detectors. Disc integrators were employed in early work (procedure 1) and a Hewlett-Packard 3390A electronic integrator for most of the experiments described in this paper (procedure 2). In procedure 1 matched $^1/_8$ in. × 3.5 ft columns packed with 5% Apiezon M on Chromosorb W were employed with column and injector temperatures at 170 °C. In procedure 2 a 50-m Altech FSOT-1, OV-1 (poly(dimethylsiloxane)) coated capillary column was employed; injector, column, and detector temperatures were 200–225, 210, and 275 °C, respectively. Benzophenone or stilbene was used as an internal standard and control injections showed that A_2, Ad, and A_2d do not split to A under these conditions. Except as noted in the results section, the same results were obtained for adduct yields from the two procedures. The capillary GLC column was also employed for stilbene actinometer analyses at the later stages of this work.

Isotope Dilution Analysis (IDA). Reverse IDA[65] was employed to determine yields of A_2 and A_2d. Generally sets of 6 or more ampules (6-mL aliquot of A-^{14}C solution/ampule) were irradiated in the merry-go-round apparatus (see irradiation procedures). Loss of A was monitored periodically by UV with use of a Pyrex cell attached to one of the ampules. Irradiations were terminated at <30% loss of A. Samples were allowed to undergo thermal Diels–Alder reaction in the dark (with heating to 60–70 °C, as necessary) until no more A loss could be observed by UV. Samples were then opened to air, each set was combined, and known quantities of A_2-^{12}C and A_2d-^{12}C (weights were in the 20–50-mg

(62) Fieser, L. F.; Williamson, K. L. *Organic Experiments*, 4th ed.; Heath: Lexington, MA, 1979; p 260.
(63) Metts, L.; Saltiel, J., unpublished results.
(64) Saltiel, J.; Townsend, D. E.; Sykes, A. *J. Am. Chem. Soc.* **1973**, *95*, 5968.
(65) Tolgyssey, J.; Braun, T.; Kyrs, M. *Isotope Dilution Analysis*; Pergamon Press: New York, 1972.

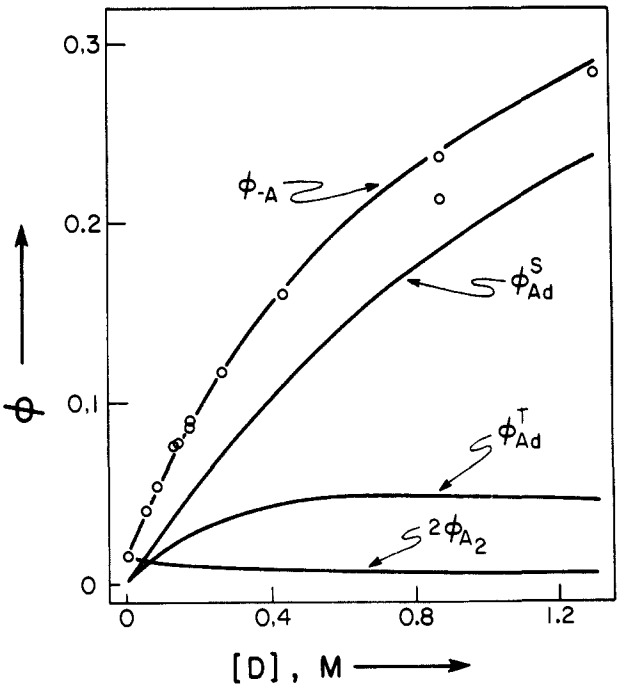

Figure 8. Diene concentration dependence of ϕ_{-A} and calculated contributions of the three major reaction channels for low [^{1}A].

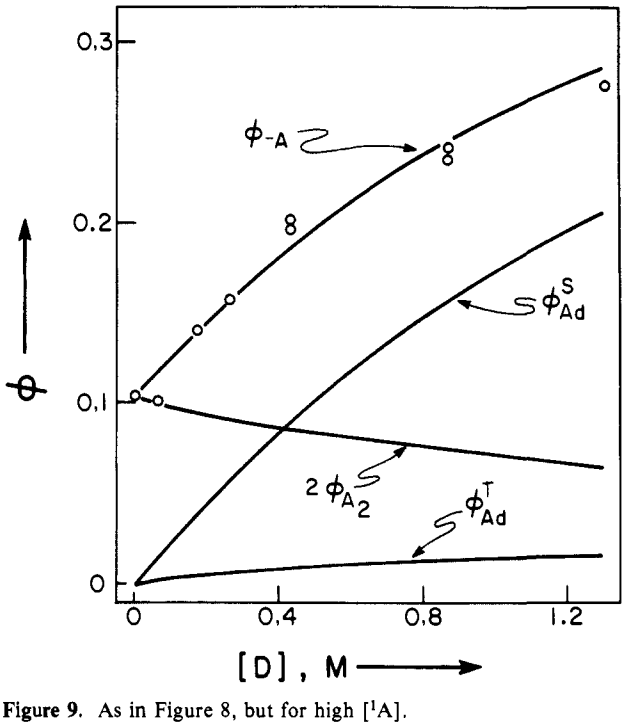

Figure 9. As in Figure 8, but for high [^{1}A].

range) were dissolved in the mixture. Homogenization of the solution was ensured by addition of benzene as needed. Benzene and diene were removed on the rotary evaporator, *n*-hexane was added to the solid residue, and the mixture was warmed gently until all A_2d dissolved (A_2 is essentially insoluble in *n*-hexane). A_2 was filtered out and the filtrate containing A_2d and unreacted A was irradiated under Ar (Uranyl glass filter—450 W Hanovia Hg lamp) until all A-^{14}C dimerized (UV). This second dimer was filtered out and discarded; the filtrate was concentrated and upon standing A_2d crystallized. Recrystallization of isolated A_2 and A_2d from benzene and *n*-hexane, respectively, led to A-^{14}C-free A_2 and A_2d (UV). Known quantities (5–9 mg) of purified A_2 and A_2d were dissolved in 50.0 mL of POP and POPOP solution (2.00 g of POP, 24.0 mg of POPOP to 250 mL with benzene). Scintillation counting was performed (Beckman LS-250 Liquid Scintillation System) on 20.0-mL aliquots for 5-min intervals. With each experiment a standard solution containing undiluted A_2-^{14}C was also counted (~11,600 cts/mg vs. ~65 cts/mg for background). The activity of undiluted A_2d-^{14}C, ~9,400 cts/mg, was obtained by multiplying the A_2-^{14}C value by the molecular weight ratio. It was shown that the specific activity of A_2-^{14}C is independent of the mass of A_2-^{14}C used in the range employed in these experiments. Specific activities of diluted A_2-^{14}C and A_2d-^{14}C were used to calculate yields of A_2 and *t*-[4,4]Ad, respectively. In several instances excellent agreement was achieved between duplicate experiments.

Quantum Yield Measurements. The main departure from previous work[5,27,48] was the use of attached UV cells on selected ampules so that A loss could be followed without opening solutions to air. The filters used to isolate the group of Hg lines at 366 nm and the filter solution used to isolate 404- and 436-nm lines have been described (see Filter 1 and Filter 2 in ref 48). Actinometer conversions to *cis*-stilbene were corrected for zero time *cis*-stilbene content and back reaction.[20] Values of 59.2% (0.55) and 86.0% *cis*-stilbene (0.47) were employed as photostationary compositions (and $\phi_{t\rightarrow c}$ quantum yields) for benzophenone and fluorenone sensitization, respectively.[18-20,22] For the lowest [A] solutions a small correction (2–5%) was applied on quantum yields to account for incomplete light absorption by A ($\epsilon_{366} = 2.71 \times 10^3$ M^{-1} cm^{-1}). Irradiated ampules were degassed with 5 freeze–pump–thaw cycles to 10^{-6} torr and flame sealed at a constriction. Air-saturated samples were loosely sealed with standard taper 10/30 glass stoppers during the irradiation period.

Adduct Preparation. Preparative scale irradiations were carried out in cylindrical Pyrex Hanovia reactors (0.2–2.0-L capacity) equipped with water-cooled Pyrex lamp probes, Hanovia medium-pressure 200 or 450 W Hg lamps, and fritted glass bubblers. Irradiation was mainly through a Uranyl glass filter ($\lambda > 320$ nm) for direct excitation experiments or xanthone-sensitized conversion of *t*-[4,4]Ad to *c*-[4,4]Ad and through a filter solution ($\lambda = 404$, 436 nm—Filter 2 ref 48) for fluorenone-sensitized adduct formation. A constant stream of Ar or N_2 gas was bubbled through the solution during the irradiation, and the progress of the reaction was checked periodically by UV. Photoadduct separation was by chromatography on alumina as previously reported,[14,16] except that, in our hands, *t*-[4,4]Ad did not survive the chromatography procedure. ^{1}H NMR spectra of *t*-[4,4]Ad, *c*-[4,4]Ad, and [2,4]Ad agreed with those previously reported.[14,16] Spin decoupling ^{1}H NMR experiments generally agreed with previous peak assignments.[21] A_2d prepared by the thermal addition of A to *t*-[4,4]Ad was purified by recrystallization from *n*-hexane, mp 336–338 °C, and its structure established by X-ray crystallography as described below.

X-ray Structure Determination of A_2d. Preliminary examination of the A_2d crystal on the diffractometer showed monoclinic symmetry. The systematic absences indicated the space group $P2_1/c$. Cell constants at 22 ± 1 °C from the computer centering and least-squares fit of the angular settings of 25 reflections within 2θ limits of $16° < 2\theta < 34°$ were the following $a = 9.894$ (4) Å, $b = 16.021$ (3) Å, $c = 15.798$ (4) Å, $\beta = 108.45$ (3)°, $V = 2375.5$ Å^3, $d_{calcd} = 1.226$ g/cm^3, $d_{obsd} = 1.21$ g/cm^3, with $Z = 4$.

The data were collected on an Enraf-Nonius CAD4 diffractometer with use of Mo Kα radiation ($\lambda = 0.71073$ Å) and a graphite crystal incident beam monochromater. A total of 4745 reflections in the range $0° < 2\theta < 50°$ were collected. The intensities of three standard reflections were measured every 2 h; no crystal decomposition during the data collection was observed. After data reduction, averaging equivalent reflections, and rejecting systematically absent reflections, 1873 reflections with $|F_{obsd}| > 3\sigma_F$ remained and were used to solve and refine the structure.

Solution and refinement proceeded smoothly. The structure was solved by direct methods[66] and refined by full-matrix least-squares procedures.[67] All non-hydrogen atoms were located and refined anisotropically. The positions of hydrogen atoms were then calculated assuming typical C–H (0.95 Å) distances and idealized geometry. The final cycles of refinement, with the hydrogen atoms included with fixed positional and thermal parameters, converged to $R_1 = 7.7\%$ and $R_2 = 8.8\%$ for the 1873 observed reflections. A final difference map was featureless with maximum electron density of 0.3 e/Å^3.

Acknowledgment. This work was supported by NSF Grants GP-24265, CHE 80-26701, and CHE 84-00706.

Supplementary Material Available: Thermal parameters for carbon atoms and positional parameters for hydrogen atoms in A_2d (Tables I-S and II-S, respectively) and the effect of Az on A fluorescence (Table III-S) (3 pages). Ordering information is given on any current masthead page.

(66) MULTAN 78 "A System of Computer Programmes for the Automatic Solution of Crystal Structures from X-Ray Diffraction Data." Peter Main, Department of Physics, University of York, York, England.

(67) All programs were from the Structure Determination Programs package purchased from the Enraf-Nonius Corp. All computations and plots were done on a PDP 11/34 computer.